Top EFT Fits

Jon S. Wilson
on behalf of the ATLAS and CMS Collaborations

Baylor University

15th International Workshop on Top-Quark Physics
6 September 2022

- Effective Field Theory (EFT) is a model-independent approach to physics beyond the standard model
- Assume that new physics exists at some scale Λ beyond the current reach of experiments
- Enumerate all possible terms in the Lagrangian, ordered by their mass dimension
- Multiply terms up to some maximum mass dimension by vector of Wilson coefficients
- SM corresponds to all c_i at zero
- Analyses measure coefficients

The EFT Langrangian

$$\mathcal{L} = \mathcal{L}_{\mathrm{SM}} + \sum_{d=5}^{\infty} \sum_{i} \frac{1}{\Lambda^{d-4}} c_i^{(d)} \mathcal{O}_i^{(d)}$$

where d is the mass dimension, $c_i^{(d)}$ is a Wilson coefficient, and $\mathcal{O}_i^{(d)}$ is an operator

Historical / other EFTs include

- Fermi's theory of beta decay
- BCS theory of superconductivity
- many others, especially in condensed matter physics

- The EFT most useful for top quark physics at the LHC is the standard model EFT, or SMEFT
- Usually look at dimension-6 operators
  - The SM already contains dimension-2 and -4 operators
  - Only one dimension-5 operator exists, which provides neutrino mixing
  - The fun stuff starts at dimension-6
- Need a useful basis for the vector space of dim-6 Wilson coefficients
- Most commonly used is "Warsaw basis" [JHEP 10 (2010) 085]
- 63 total operators, of which 4 produce baryon-number violation
  - Many times more operators when considering all possible flavors
- Other bases sometimes used when more convenient for specific analyses
- For more information about EFT fits beyond the top sector, see the next two talks

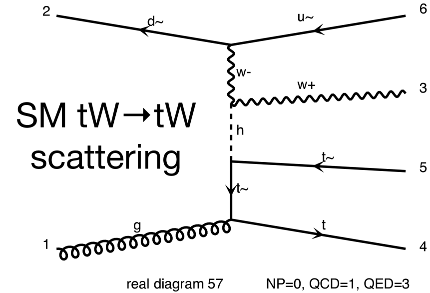

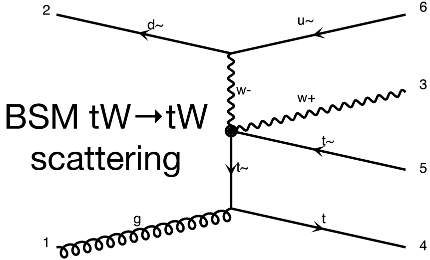

- Operators may alter rates/spectra for SM processes directly or via interference (diagrams on left)
- Or allow SM-forbidden processes (below)
- Make precision top measurements and perform searches involving top to constrain top-related WCs

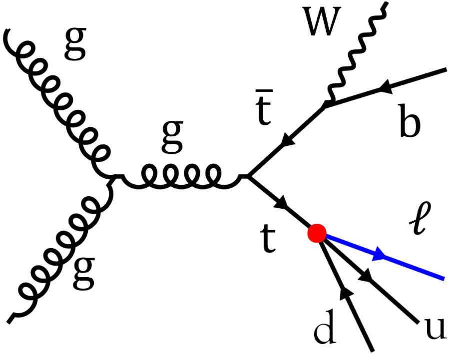

- Assume Wilson coefficients small enough to be perturbative
- At leading order in EFT:
  - Scattering amplitudes linear in coefficients
  - Cross sections quadratic in coefficients
  - SMEFT@NLO: NLO in SM, still LO in EFT
- Produce S_0, $S_{1,i}$, and $S_{2,ij}$ fit templates
  - Total $(N+1)(N+2)/2$ for N coefficients, per affected process
  - Scale them with coefficients
- But, HEP fit tools use cross sections directly as parameters of interest
  - Assume linear scaling of templates
  - Need modified tools for EFT fits

$$\sigma_{\mathrm{EFT}}\left(\frac{c_i}{\Lambda^2}\right) = S_0 + \sum_i S_{1,i}\frac{c_i}{\Lambda^2} + \sum_{i,j} S_{2,ij}\frac{c_i c_j}{\Lambda^4}$$

- S_0: SM cross section
- $S_{1,i}$: interference between SM and EFT
- $S_{2,ij}$: cross section from single EFT operator (for $i=j$) or interference between EFT operators (for $i \neq j$)

Two broad approaches to EFT fits:

Reinterpretation of unfolded measurements	Fully-simulated EFT throughout analysis
✓Can be done outside experiment	✗Must be done by experiments
✓Easier to do combinations	✗Combinations more difficult
✗No EFT acceptance effects	✓EFT acceptance effects can be included
✗No EFT effects on backgrounds	✓Background effects can be included

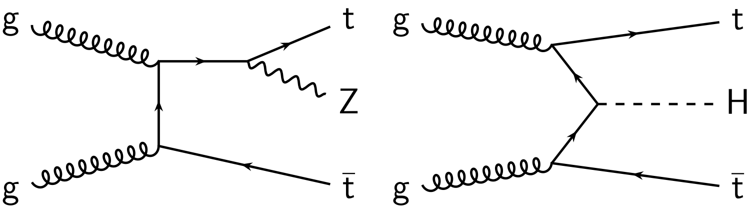

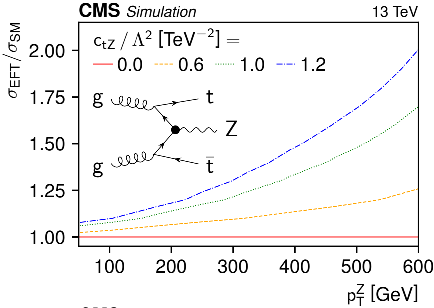

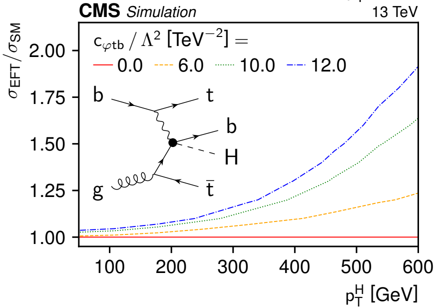

- Measure $t\bar{t}Z/t\bar{t}H$ when $p_T(Z/H)$ is large
- EFT effects more pronounced at high $p_T(Z/H)$
- Fully-simulated EFT effects on signal and $t\bar{t}+b\bar{b}$ background
- See Jan van der Linden's talk from Monday for full details

- Vary the $t\bar{t}Z/H$ signal and $t\bar{t}+b\bar{b}$ background as functions of the WCs
- Perform 1-D and 2-D likelihood scans for each WC and pair of WCs
- Consistent with SM (all WCs zero) at 95% CL
- Phase space with highly-boosted Z/H
- Complementary to other analyses
- Comparable sensitivity

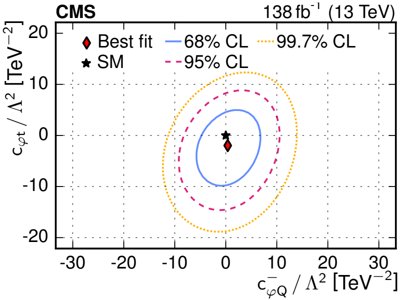

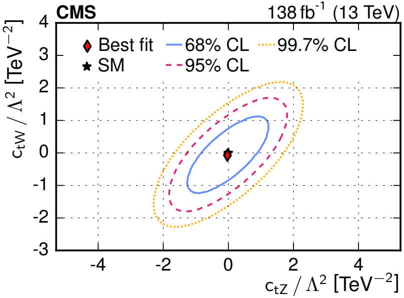

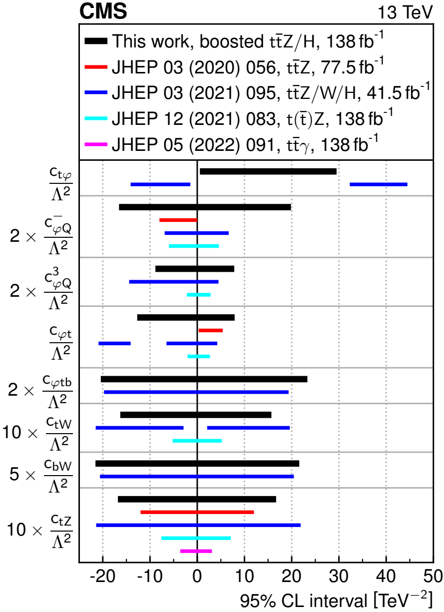

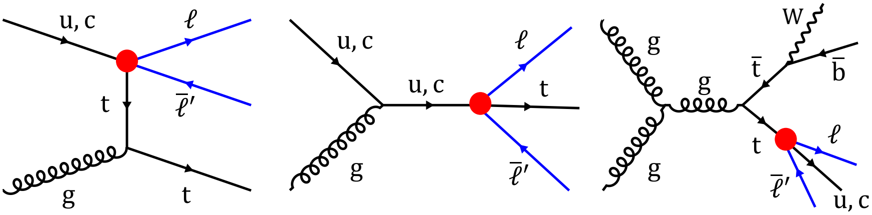

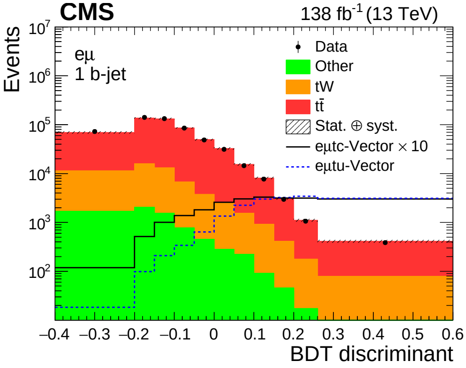

- Search for charged lepton flavor violation with top
- See Jiwon Park's talk Wednesday for full details
- $e\mu tq$ vertex in production or decay
- Forbidden in SM, so no EFT–SM interference
- Fully-simulated EFT signals
- Use a BDT to separate signal from BG
  - $e\mu tc$ and $e\mu tu$ very similar shapes

- No sign of charged lepton flavor violation
- Exclusion in $c_{e\mu tc}$-$c_{e\mu tu}$ plane above and right of curves
- Scalar, vector, and tensor variants contribute differently to production vs. decay
- Near-degeneracy, plus zero interference between $e\mu tc$ and $e\mu tu$, makes exclusion curves nearly ellipses
  - Sensitive to roughly $c_{e\mu tc}^2 + c_{e\mu tu}^2$
- World's strongest limits on charged lepton flavor violation in top sector

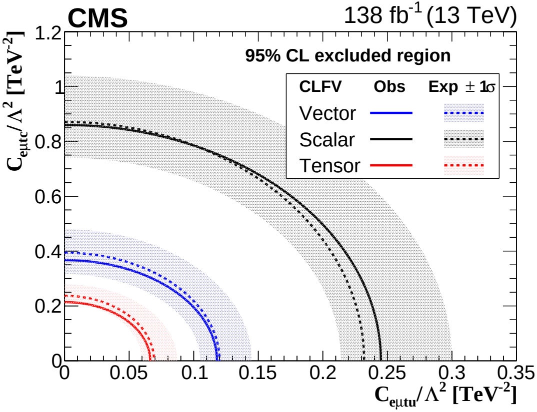

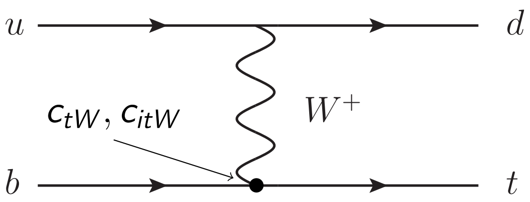

- Measure polarization of *t*-channel single top
- Lepton+jets final state
- Unfolded differential cross sections vs. $\cos\theta_{\ell x'}$, $\cos\theta_{\ell y'}$, and $\cos\theta_{\ell z'}$
  - x', y', z' coordinate system based on top quark rest frame
  - $\theta_{\ell x'}$ angle between lepton and x' direction
- Reinterpret unfolded $\cos\theta_{\ell x'}$ and $\cos\theta_{\ell y'}$ as EFT constraints on real c_{tW}, imaginary c_{itW}

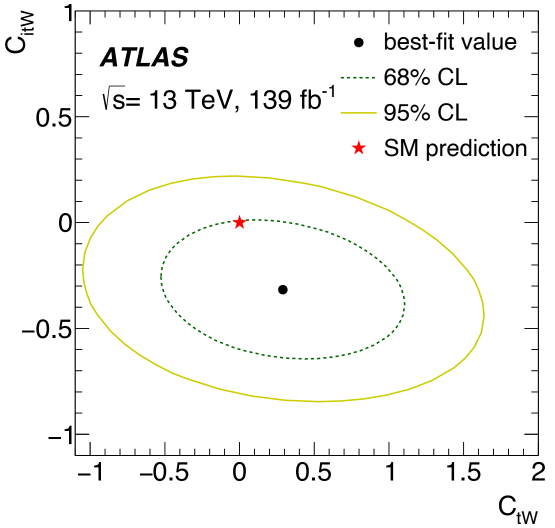

For more information, see Miriam Watson's talk this afternoon

- Two analyses measuring boosted $t\bar{t}$ differential cross sections:
  - Lepton+jets [JHEP 06 (2022) 063]
  - All-hadronic [arXiv:2205.02817]
- Unfold differential cross section to parton level
- Several kinematic variables measured
- Top quark p_T used for EFT constraints
  - p_T of the hadronic top in lepton+jets analysis
  - p_T of leading top in all-hadronic analysis
- EFT constraints as reinterpretations of unfolded differential cross sections
- Covered in more detail on Monday by Peter Hansen; see also poster by Jonathan Jamieson

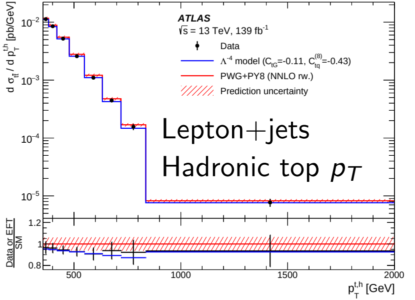

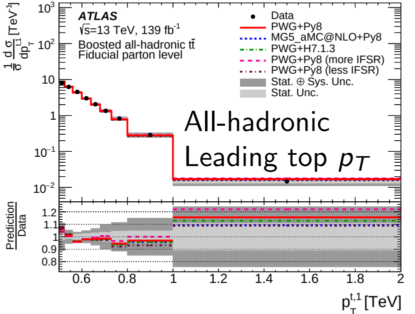

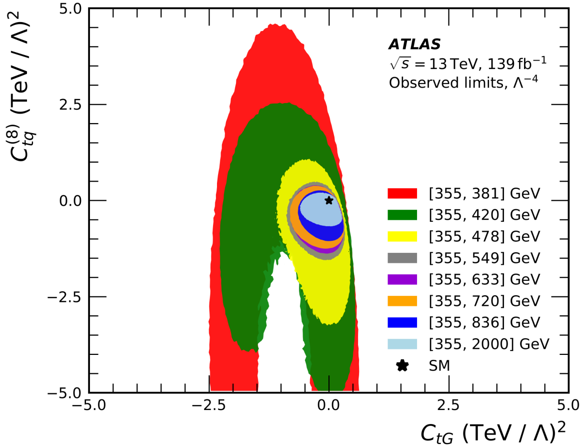

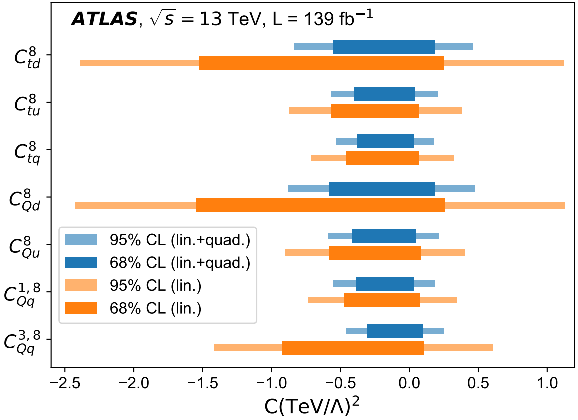

Lepton+jets:

- Constraints on C_{tG} and $C_{tq}^{(8)}$
- Consistent with SM at 68 % CL

All-hadronic:

- Constraints on seven four-quark operators
- Consistent with SM at 68 % CL

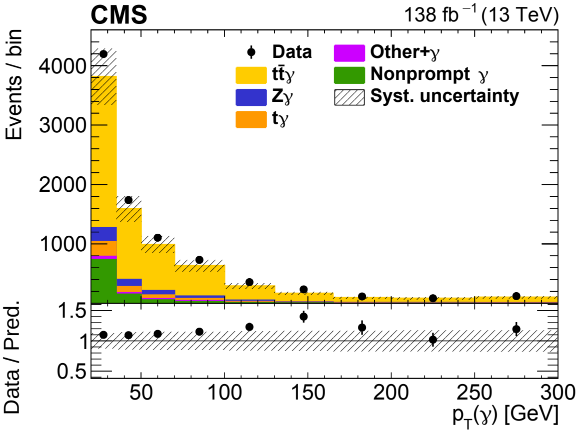

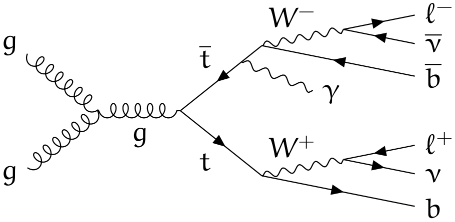

- $t\bar{t}\gamma$ production in dilepton final state
- Measure differential cross section as function of $p_T(\gamma)$
- See Jan van der Linden's talk from Monday for full details
- Fully-simulated EFT effects on $t\bar{t}\gamma$

- Differential cross section used to constrain Wilson coefficients c_{tZ} and c^{I}_{tZ}
- WCs $c_{t\gamma}$ and $c^{I}_{t\gamma}$ also explored, but are degenerate with c_{tZ}/c^{I}_{tZ} in this analysis
- 1-D and 2-D likelihood scans; showing 2-D scan here
- Combine result with JHEP 12 (2021) 180: $t\bar{t}\gamma$ in lepton+jets final state
- Results consistent with the SM

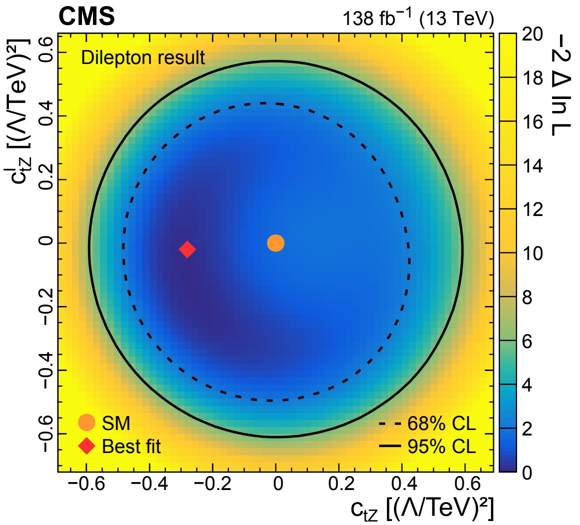

- Differential cross section used to constrain Wilson coefficients c_{tZ} and c^{I}_{tZ}
- WCs $c_{t\gamma}$ and $c^{I}_{t\gamma}$ also explored, but are degenerate with c_{tZ}/c^{I}_{tZ} in this analysis
- 1-D and 2-D likelihood scans; showing 2-D scan here
- Combine result with JHEP 12 (2021) 180: $t\bar{t}\gamma$ in lepton+jets final state
- Results consistent with the SM

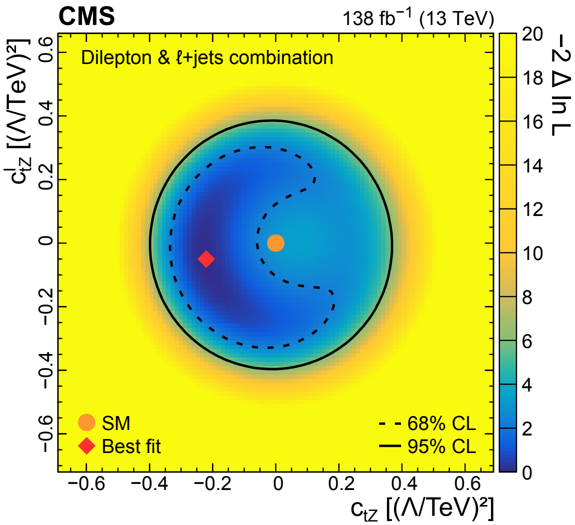

- Measure top asymmetries:
  - $t\bar{t}$ Rapidity asym. $A_C^{t\bar{t}} \equiv A(|y_t| - |y_{\bar{t}}|)$: [arXiv:2208.12095]
  - $t\bar{t}j$ Energy asym. $A_E \equiv A(E_t - E_{\bar{t}})$: [EPJC 82 (2022) 374]
- Where

$$A(X) = \frac{N(X > 0) - N(X < 0)}{N(X > 0) + N(X < 0)}$$

- Unfold:
  - $A_C^{t\bar{t}}$ vs. $m_{t\bar{t}}$
  - A_E vs. angle of additional jet θ_j
- Constrain fifteen ($A_C^{t\bar{t}}$) or six (A_E) coefficients by reinterpreting unfolded double-differential cross sections

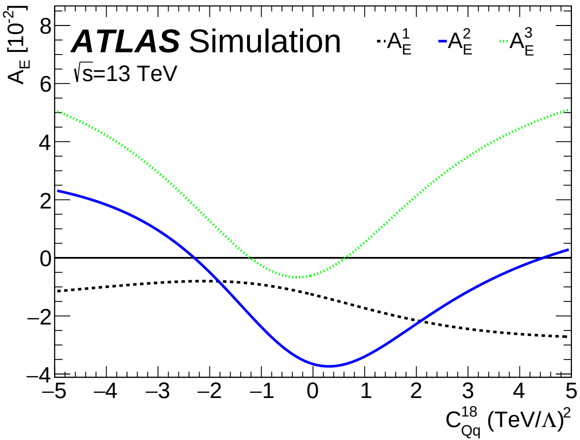

- See talk by Barbora Eckerova this afternoon for more details

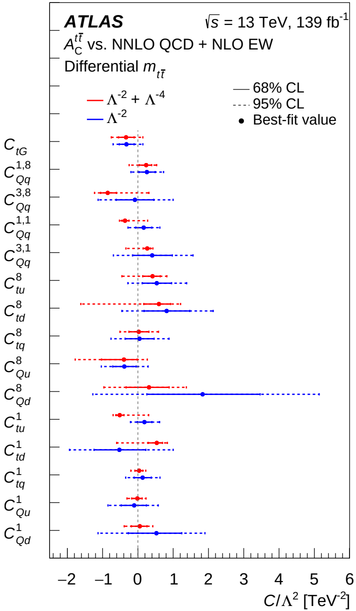

- Coefficient constraints from $A_C^{t\bar{t}}$ vs. $m_{t\bar{t}}$ (left)
- Compared to A_E coefficient constraints (right)
  - $A_C^{t\bar{t}}$ in red
  - A_E in blue
- $A_C^{t\bar{t}}$, A_E complement nicely
- A_E requires additional jet
  - QCD structure different, so different EFT effects
- Shows importance of EFT combinations

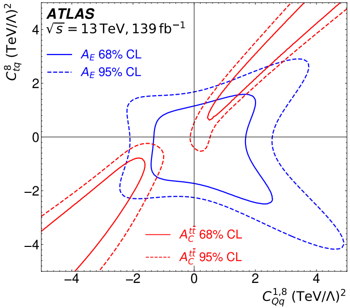

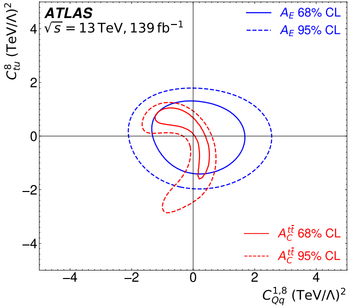

- EFT is a powerful tool for studying the dynamics of the top sector and searching for new physics
- Many strategies/techniques for EFT fits
- Combinations of complementary analyses crucial for future sensitivity to possible new physics
- CMS and ATLAS producing wide range of top EFT fits
  - Boosted $t\bar{t}Z/H$
  - SM-forbidden processes: charged-lepton flavor violation and flavor-changing neutral currents
  - Differential cross sections for $t\bar{t}\gamma$ and $t\bar{t}$
  - Polarization of single top
  - Charge and energy asymmetry of $t\bar{t}$

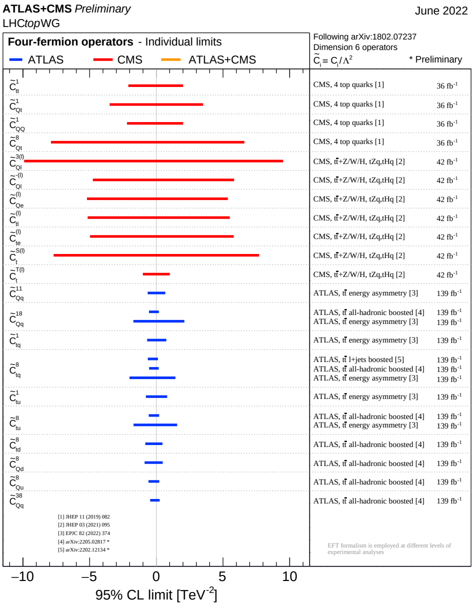

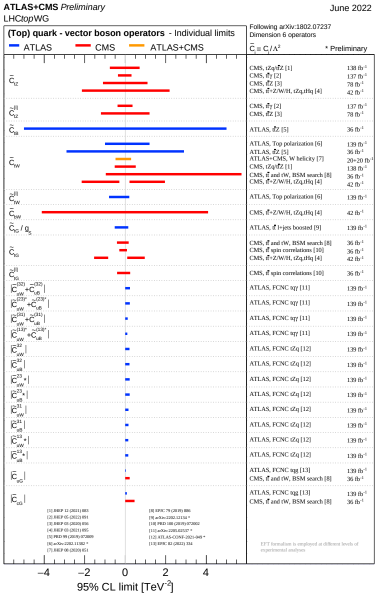

ATLAS+CMS Preliminary
LHCtopWG
June 2022
(Top) quark - vector boson operators - Individual limits
ATLAS
CMS
ATLAS+CMS
Following arXiv:1802.07237
Dimension 6 operators
C̃ ≡ C / Λ²
* Preliminary
CMS, tZq/tt̄Z [1] 138 fb⁻¹
CMS, tt̄γ [2] 137 fb⁻¹
CMS, tt̄Z [3] 78 fb⁻¹
CMS, tt̄+Z/W/H, tZq,tHq [4] 42 fb⁻¹
ATLAS, tt̄Z [5] 36 fb⁻¹
ATLAS, Top polarization [6] 139 fb⁻¹
ATLAS+CMS, W helicity [7] 20+20 fb⁻¹
CMS, tt̄ and tW, BSM search [8] 36 fb⁻¹
ATLAS, tt̄ l+jets boosted [9] 139 fb⁻¹
CMS, tt̄ spin correlations [10] 36 fb⁻¹
ATLAS, FCNC tqγ [11] 139 fb⁻¹
ATLAS, FCNC tZq [12] 139 fb⁻¹
ATLAS, FCNC tqg [13] 139 fb⁻¹
[1] JHEP 12 (2021) 083
[2] JHEP 05 (2022) 091
[3] JHEP 03 (2020) 056
[4] JHEP 03 (2021) 095
[5] PRD 99 (2019) 072009
[6] arXiv:2202.11382 *
[7] JHEP 08 (2020) 051
[8] EPJC 79 (2019) 886
[9] arXiv:2202.12134 *
[10] PRD 100 (2019) 072002
[11] arXiv:2205.02537 *
[12] ATLAS-CONF-2021-049 *
[13] EPJC 82 (2022) 334
EFT formalism is employed at different levels of experimental analyses
−4
−2
0
2
4
95% CL limit [TeV⁻²]

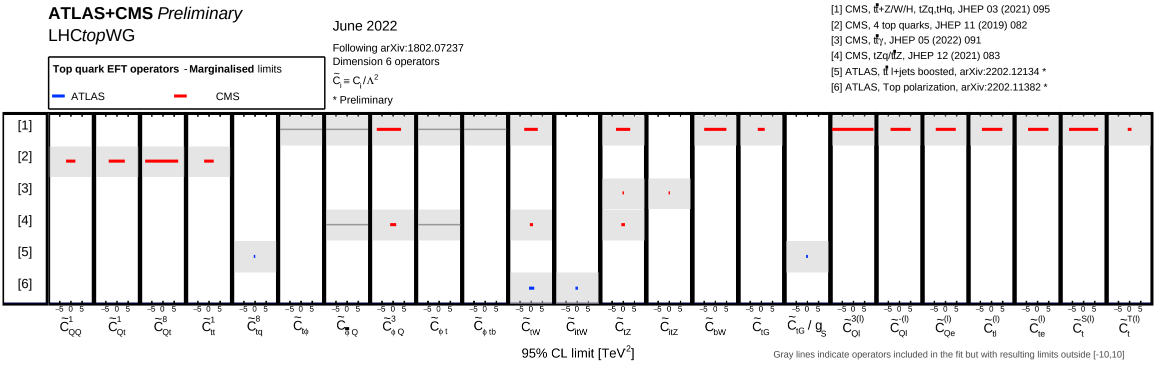
ATLAS+CMS Preliminary
LHCtopWG
June 2022
Following arXiv:1802.07237
Dimension 6 operators
* Preliminary
Top quark EFT operators - Marginalised limits
ATLAS
CMS
[1] CMS, tt̄+Z/W/H, tZq,tHq, JHEP 03 (2021) 095
[2] CMS, 4 top quarks, JHEP 11 (2019) 082
[3] CMS, tt̄γ, JHEP 05 (2022) 091
[4] CMS, tZq/tt̄Z, JHEP 12 (2021) 083
[5] ATLAS, tt̄ l+jets boosted, arXiv:2202.12134 *
[6] ATLAS, Top polarization, arXiv:2202.11382 *
95% CL limit [TeV^2]
Gray lines indicate operators included in the fit but with resulting limits outside [-10,10]

Backup: ATLAS FCNC

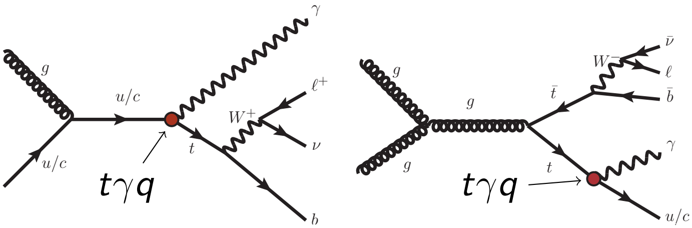

- Search for flavor-changing neutral currents in two analyses:
  - tHq vertex, decay only, $H \to \tau\tau$ [arXiv:2208.11415]
  - $t\gamma q$ vertex, production and decay [arXiv:2205.02537]
- SM-forbidden processes
- Fully-simulated EFT signals
- Both analyses use multivariate analyses
- Backgrounds constrained using control regions
- See Wednesday talk by Lucio Cerrito for more details

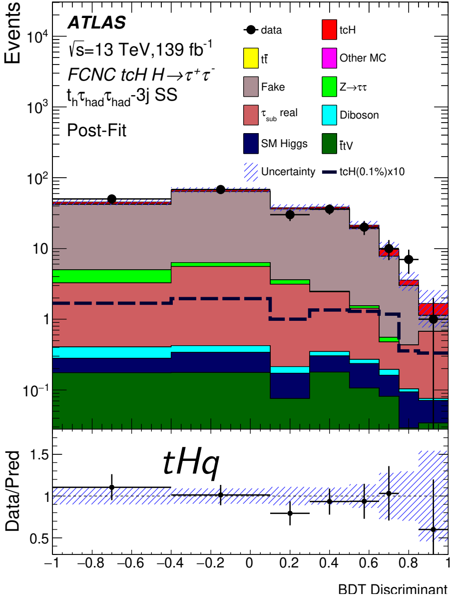

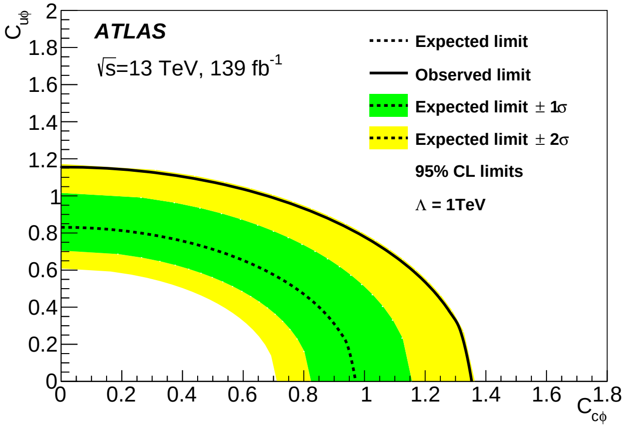

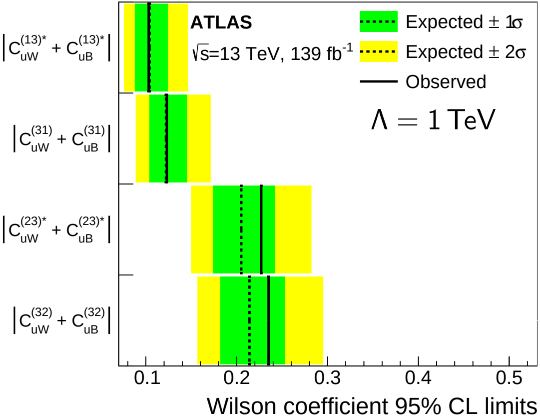

tHq search:

- Constraints on $c_{c\phi}$ and $c_{u\phi}$
- Excluded region is above/right of curves
- Modest excess, local significance 2.3σ

$t\gamma q$ search:

- Constraints on linear combinations of pairs of FCNC operators
- Excluded region to the right

Backup: Boosted $t\bar{t}Z/H$

- NN trained to distinguish $t\bar{t}Z/H$ from backgrounds

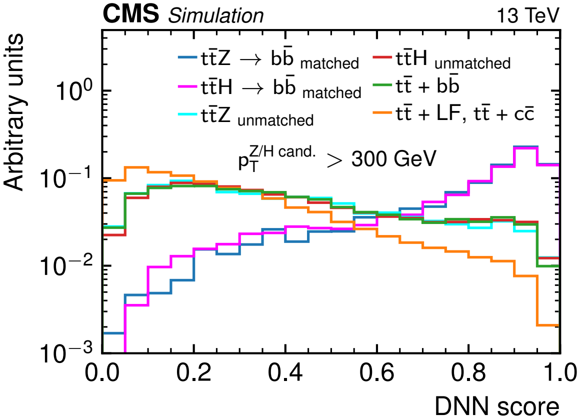

- Divide events among bins as functions of NN score, Z/H jet mass, and $p_T(Z/H)$
  - $p_T(Z/H)$ provides EFT sensitivity
  - NN score provides a high-purity region
  - Z/H jet mass provides sidebands to help control backgrounds

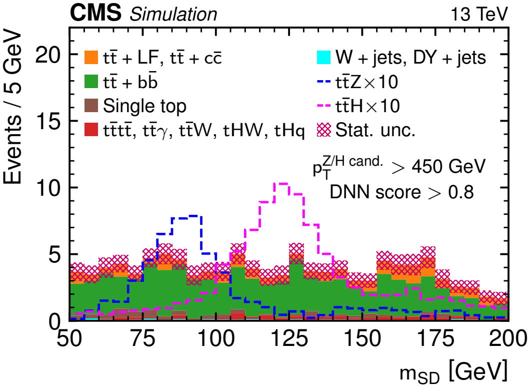

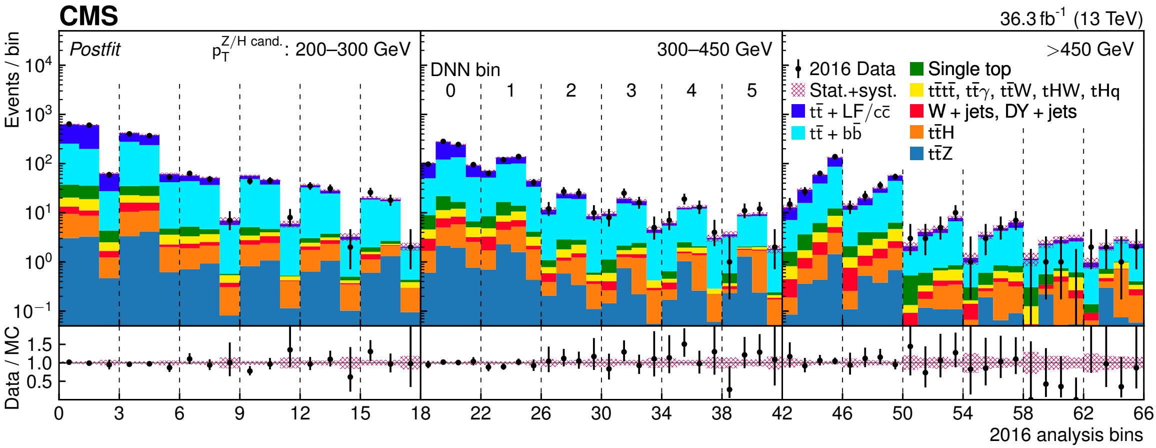

- Showing 2016 data as an example
- fit to all three years simultaneously
- 3 large groups: $p_T(Z/H)$ bins
- 6 medium subgroups: NN bins
- Individual bins: Z/H jet mass bins
- Use this, plus 2017/18, to constrain WCs

Operator	Definition	WC
$^{\ddagger}O_{u\varphi}^{(ij)}$	$\bar{q}_i u_j \tilde{\varphi}\,(\varphi^{\dagger}\varphi)$	$c_{t\varphi} + i c_{t\varphi}^{I}$
$O_{\varphi q}^{1(ij)}$	$(\varphi^{\dagger} i\overleftrightarrow{D}_{\mu}\varphi)(\bar{q}_i\gamma^{\mu}q_j)$	$c_{\varphi Q}^{-} + c_{\varphi Q}^{3}$
$O_{\varphi q}^{3(ij)}$	$(\varphi^{\dagger} i\overleftrightarrow{D}_{\mu}^{I}\varphi)(\bar{q}_i\gamma^{\mu}\tau^{I}q_j)$	$c_{\varphi Q}^{3}$
$O_{\varphi u}^{(ij)}$	$(\varphi^{\dagger} i\overleftrightarrow{D}_{\mu}\varphi)(\bar{u}_i\gamma^{\mu}u_j)$	$c_{\varphi t}$
$^{\ddagger}O_{\varphi ud}^{(ij)}$	$(\tilde{\varphi}^{\dagger} iD_{\mu}\varphi)(\bar{u}_i\gamma^{\mu}d_j)$	$c_{\varphi tb} + i c_{\varphi tb}^{I}$
$^{\ddagger}O_{uW}^{(ij)}$	$(\bar{q}_i\sigma^{\mu\nu}\tau^{I}u_j)\,\tilde{\varphi}W_{\mu\nu}^{I}$	$c_{tW} + i c_{tW}^{I}$
$^{\ddagger}O_{dW}^{(ij)}$	$(\bar{q}_i\sigma^{\mu\nu}\tau^{I}d_j)\,\varphi W_{\mu\nu}^{I}$	$c_{bW} + i c_{bW}^{I}$
$^{\ddagger}O_{uB}^{(ij)}$	$(\bar{q}_i\sigma^{\mu\nu}u_j)\,\tilde{\varphi}B_{\mu\nu}$	$(\mathcal{C}_W c_{tW} - c_{tZ})/\mathcal{S}_W + i(\mathcal{C}_W c_{tW}^{I} - c_{tZ}^{I})/\mathcal{S}_W$

Missing transverse momentum	$p_T^{miss} > 20$ GeV
=1 electron or muon	$p_T(e) > 30$ (35 GeV) in 2016 (2017 and 2018) $p_T(\mu) > 30$ GeV $\lvert\eta(e)\rvert < 2.5$, $\lvert\eta(\mu)\rvert < 2.4$
≥1 AK8 jet	$p_T > 200$ GeV, $\lvert\eta\rvert < 2.4$ $50 < m_{SD} < 200$ GeV
=1 Z or Higgs boson candidate AK8 jet	Highest $b\bar{b}$ tagger score (>0.8)
≥5 AK4 jets (may overlap AK8 jet)	$p_T > 30$ GeV, $\lvert\eta\rvert < 2.4$
≥2 b-tagged AK4 jets	Satisfy medium DeepCSV b-tag requirements ΔR(Z or Higgs boson candidate AK8 jet) > 0.8

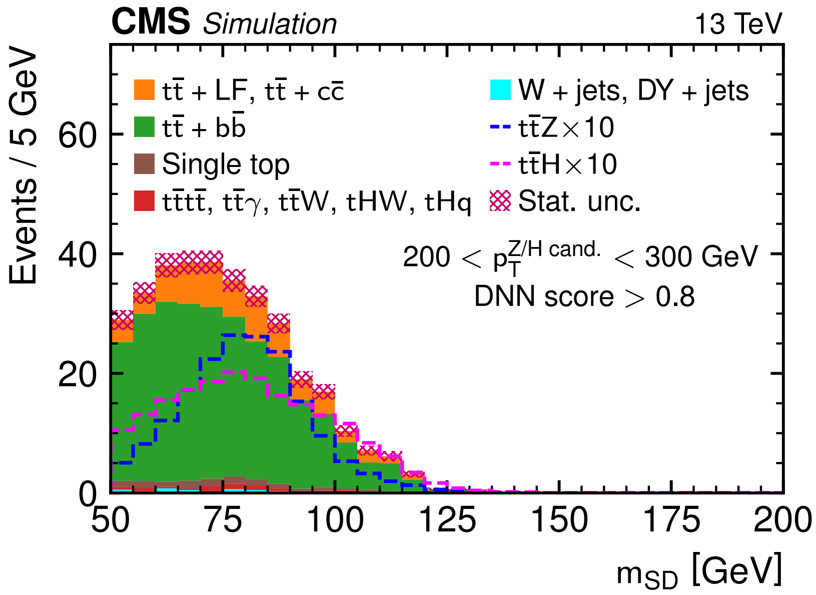
CMS Simulation
13 TeV
tt̄ + LF, tt̄ + cc̄
tt̄ + bb̄
Single top
tt̄tt̄, tt̄γ, tt̄W, tHW, tHq
W + jets, DY + jets
tt̄Z × 10
tt̄H × 10
Stat. unc.
200 < p_T^{Z/H cand.} < 300 GeV
DNN score > 0.8
Events / 5 GeV
m_SD [GeV]
0
20
40
60
50
75
100
125
150
175
200

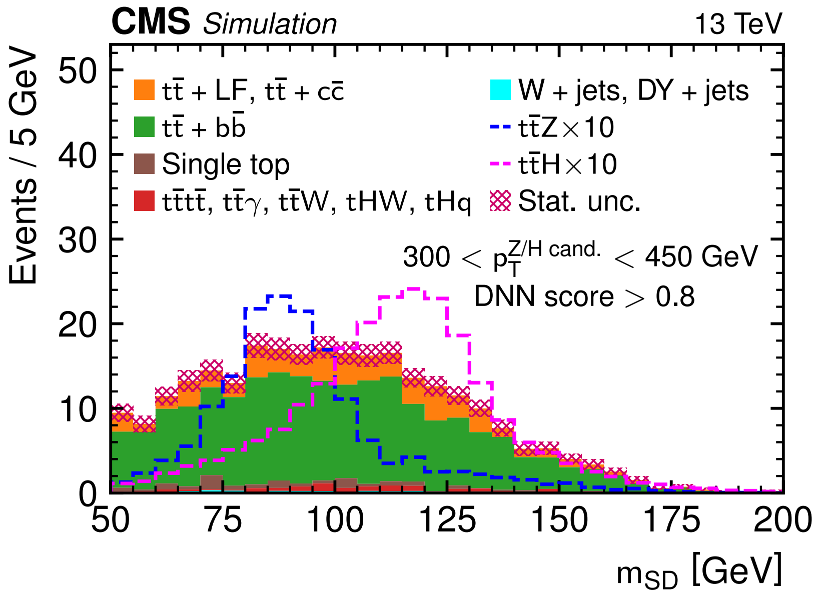
CMS Simulation
13 TeV
tt̄ + LF, tt̄ + cc̄
tt̄ + bb̄
Single top
tt̄tt̄, tt̄γ, tt̄W, tHW, tHq
W + jets, DY + jets
tt̄Z × 10
tt̄H × 10
Stat. unc.
300 < p_T^{Z/H cand.} < 450 GeV
DNN score > 0.8
Events / 5 GeV
m_SD [GeV]
0
10
20
30
40
50
50
75
100
125
150
175
200

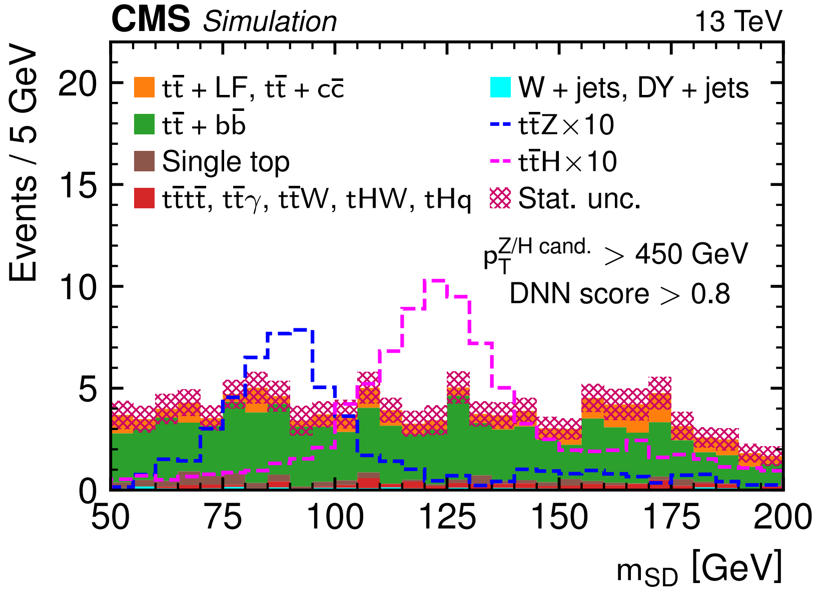
CMS Simulation
13 TeV
Events / 5 GeV
tt̄ + LF, tt̄ + cc̄
tt̄ + bb̄
Single top
tt̄tt̄, tt̄γ, tt̄W, tHW, tHq
W + jets, DY + jets
tt̄Z × 10
tt̄H × 10
Stat. unc.
p_T^{Z/H cand.} > 450 GeV
DNN score > 0.8
0
5
10
15
20
50
75
100
125
150
175
200
m_SD [GeV]

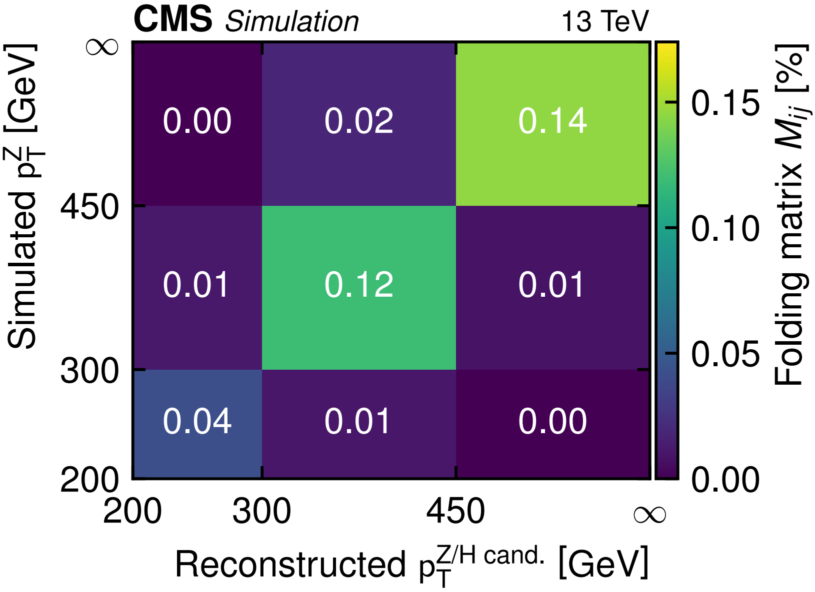
CMS Simulation
13 TeV
0.00
0.02
0.14
0.01
0.12
0.01
0.04
0.01
0.00
∞
450
300
200
200
300
450
∞
Simulated p_T^Z [GeV]
Reconstructed $p_T^{Z/H\ cand.}$ [GeV]
0.15
0.10
0.05
0.00
Folding matrix M_{ij} [%]

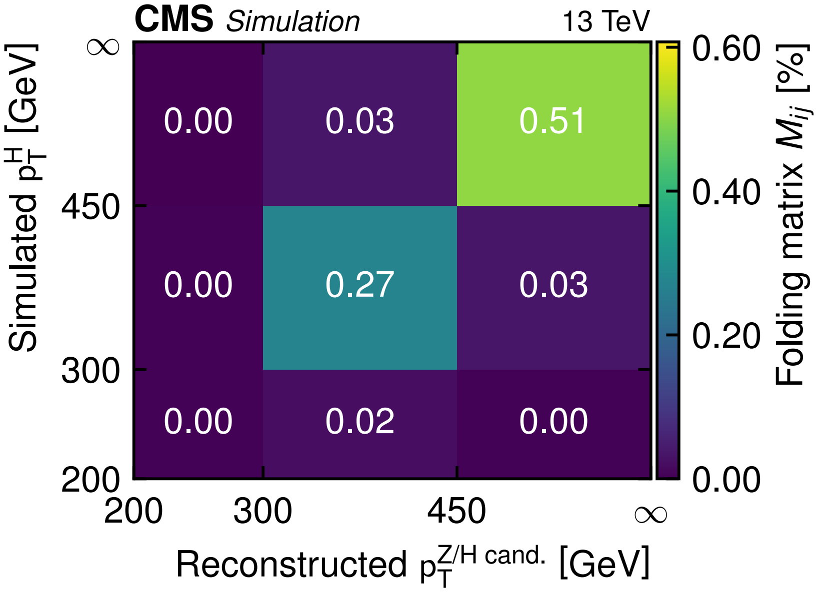

CMS Simulation
13 TeV
Simulated p_T^H [GeV]
Reconstructed $p_T^{Z/H\ cand.}$ [GeV]
Folding matrix M_{ij} [%]
0.00
0.03
0.51
0.00
0.27
0.03
0.00
0.02
0.00
200
300
450
∞
0.00
0.20
0.40
0.60

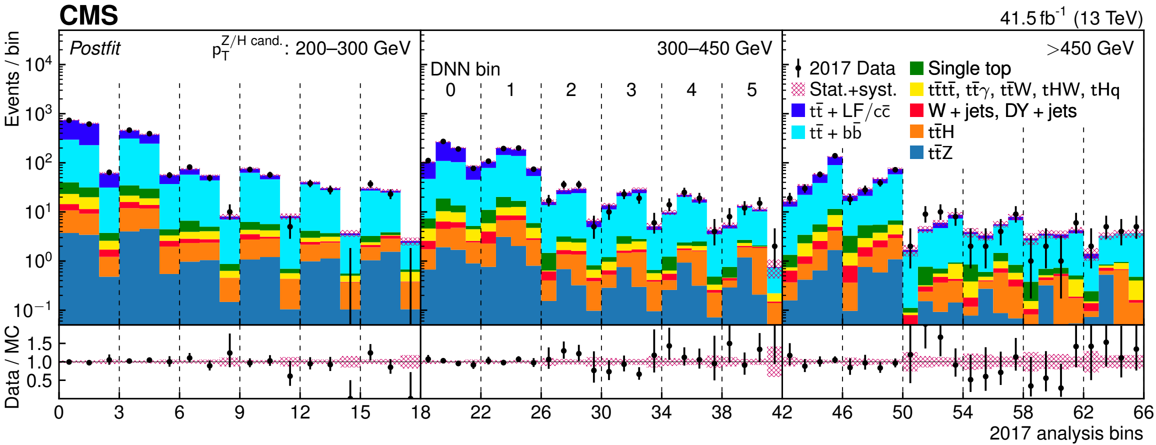
CMS
41.5 fb-1 (13 TeV)
Postfit
pT Z/H cand.: 200–300 GeV
300–450 GeV
>450 GeV
DNN bin
0 1 2 3 4 5
2017 Data
Stat.+syst.
tt̄ + LF/cc̄
tt̄ + bb̄
Single top
tt̄tt̄, tt̄γ, tt̄W, tHW, tHq
W + jets, DY + jets
tt̄H
tt̄Z
Events / bin
Data / MC
2017 analysis bins

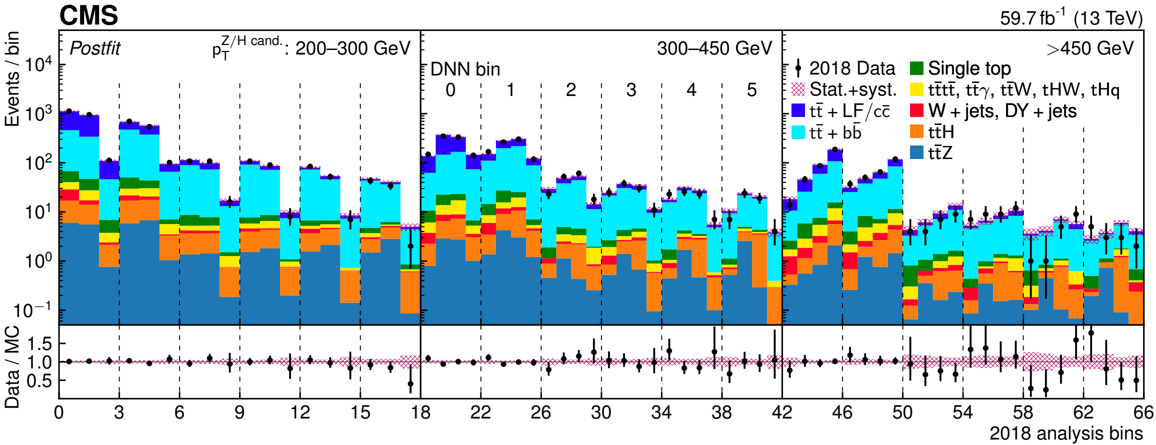
CMS
59.7 fb-1 (13 TeV)
Postfit
pT Z/H cand.: 200–300 GeV
300–450 GeV
>450 GeV
DNN bin
0 1 2 3 4 5
2018 Data
Stat.+syst.
tt̄ + LF/cc̄
tt̄ + bb̄
Single top
tt̄tt̄, tt̄γ, tt̄W, tHW, tHq
W + jets, DY + jets
tt̄H
tt̄Z
Events / bin
Data / MC
2018 analysis bins

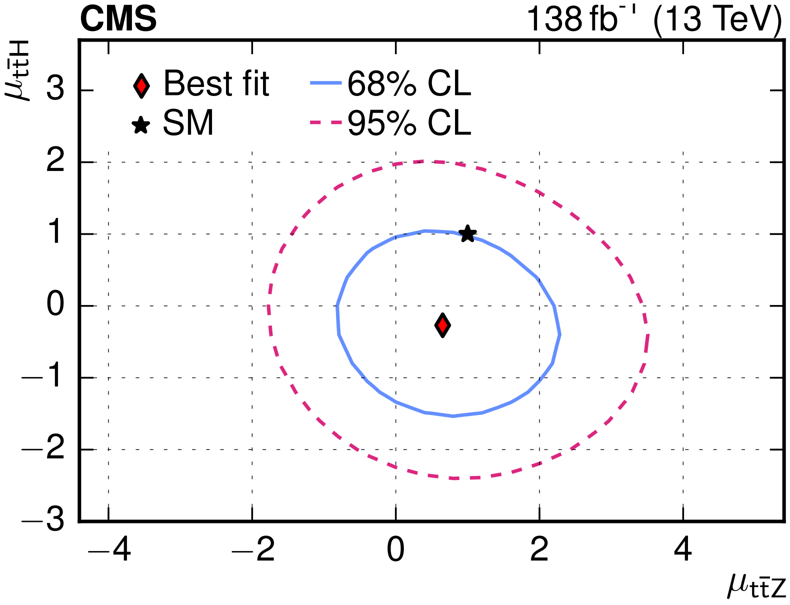
CMS
138 fb⁻¹ (13 TeV)
Best fit
SM
68% CL
95% CL
$\mu_{t\bar{t}H}$
$\mu_{t\bar{t}Z}$
3
2
1
0
−1
−2
−3
−4
−2
0
2
4

Signal strength	Observed $\pm 1\sigma$	Stat.	MC Stat.	Experiment	Theory	Expected $\pm 1\sigma$
$\mu_{\mathrm{t\bar{t}Z}}$	$0.65^{+1.05}_{-0.98}$	$^{+0.80}_{-0.76}$	$^{+0.37}_{-0.38}$	$^{+0.38}_{-0.31}$	$^{+0.42}_{-0.38}$	$1.00^{+0.92}_{-0.84}$
$\mu_{\mathrm{t\bar{t}H}}$	$-0.33^{+0.87}_{-0.85}$	$^{+0.72}_{-0.65}$	$^{+0.32}_{-0.34}$	$^{+0.19}_{-0.17}$	$^{+0.30}_{-0.38}$	$1.00^{+0.79}_{-0.73}$

Source of uncertainty	$\Delta\mu_{\mathrm{t\bar{t}Z}}$	$\Delta\mu_{\mathrm{t\bar{t}H}}$
$\mathrm{t\bar{t}}+\mathrm{c\bar{c}}$ cross section	$^{+0.24}_{-0.22}$	$^{+0.17}_{-0.16}$
$\mathrm{t\bar{t}}+\mathrm{b\bar{b}}$ cross section	$^{+0.17}_{-0.23}$	$^{+0.15}_{-0.22}$
$\mathrm{t\bar{t}}+2\mathrm{b}$ cross section	$^{+0.03}_{-0.03}$	$^{+0.10}_{-0.10}$
μ_{R} and μ_{F} scales	$^{+0.19}_{-0.14}$	$^{+0.10}_{-0.16}$
Parton shower	$^{+0.15}_{-0.16}$	$^{+0.06}_{-0.05}$
Top quark p_{T} modeling in $\mathrm{t\bar{t}}$	$^{+0.01}_{-0.01}$	$^{+0.11}_{-0.13}$
b-tag efficiency	$^{+0.25}_{-0.13}$	$^{+0.10}_{-0.11}$
$\mathrm{b\bar{b}}$-tag efficiency	$^{+0.17}_{-0.12}$	$^{+0.04}_{-0.03}$
Jet energy scale and resolution	$^{+0.11}_{-0.10}$	$^{+0.11}_{-0.12}$
Jet mass scale and resolution	$^{+0.10}_{-0.11}$	$^{+0.08}_{-0.08}$

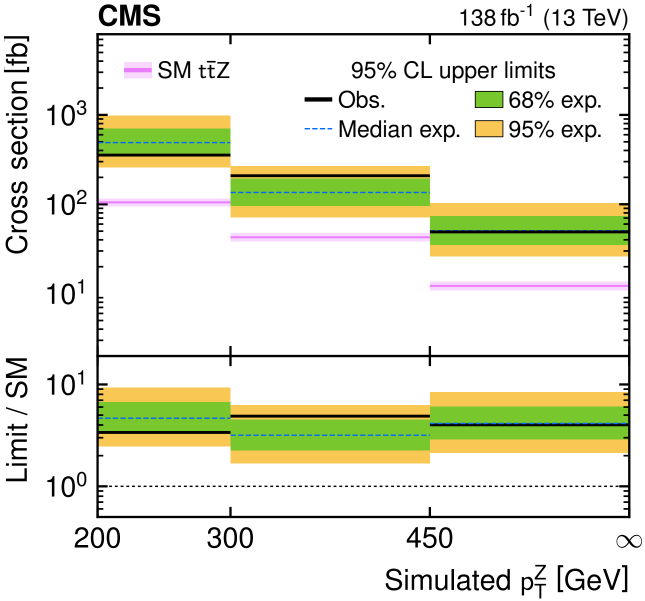
CMS
138 fb^{-1} (13 TeV)
SM tt̄Z
95% CL upper limits
Obs.
Median exp.
68% exp.
95% exp.
Cross section [fb]
10^3
10^2
10^1
Limit / SM
10^1
10^0
200
300
450
∞
Simulated p_T^Z [GeV]

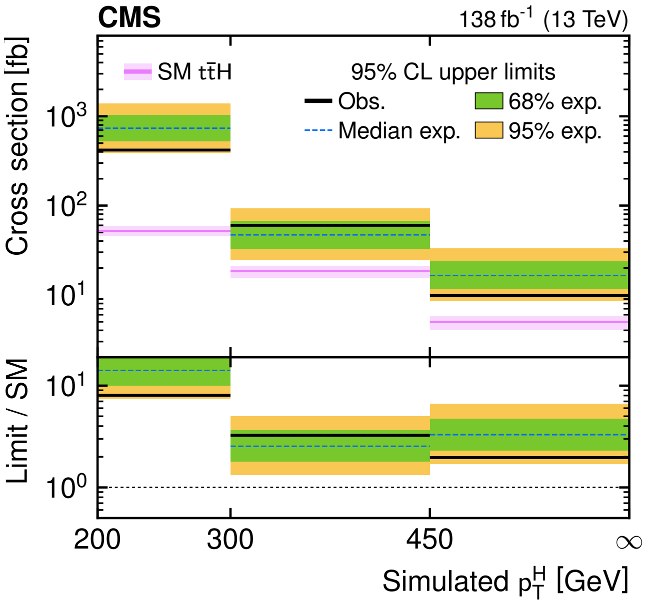
CMS
138 fb-1 (13 TeV)
SM tt̄H
95% CL upper limits
Obs.
Median exp.
68% exp.
95% exp.
Cross section [fb]
Limit / SM
Simulated pT H [GeV]
200
300
450
∞

Signal	$p_T^{Z/H}$ (GeV) interval	95% CL upper limit (fb)	95% CL upper limit / SM
$t\bar{t}Z$	(200, 300]	$359\ (492^{+216}_{-143})$	$3.42\ (4.69^{+2.06}_{-1.36})$
	(300, 450]	$208\ (135^{+58}_{-39})$	$4.88\ (3.17^{+1.37}_{-0.91})$
	$(450, \infty)$	$49.1\ (50.7^{+23.0}_{-15.4})$	$4.02\ (4.16^{+1.89}_{-1.26})$
$t\bar{t}H$	(200, 300]	$418\ (736^{+296}_{-210})$	$8.02\ (14.1^{+5.7}_{-4.0})$
	(300, 450]	$59.9\ (47.3^{+20.5}_{-13.9})$	$3.24\ (2.55^{+1.11}_{-0.75})$
	$(450, \infty)$	$9.78\ (16.5^{+7.4}_{-4.9})$	$1.96\ (3.30^{+1.49}_{-0.98})$

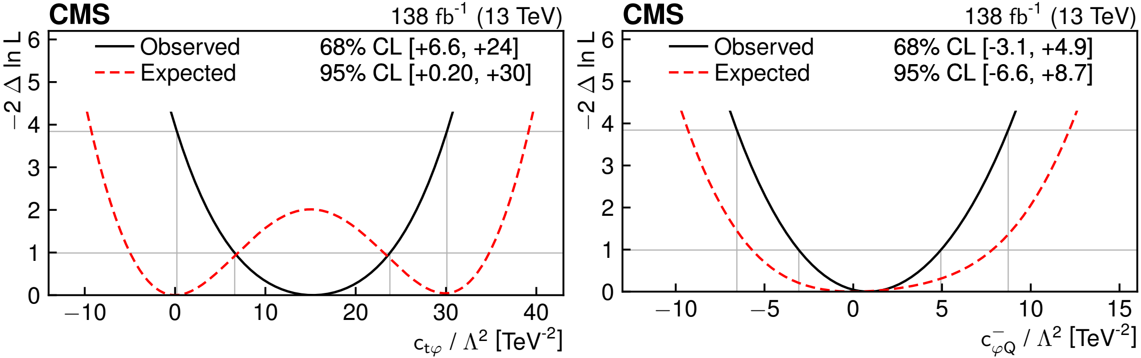
CMS
138 fb-1 (13 TeV)
Observed
Expected
68% CL [+6.6, +24]
95% CL [+0.20, +30]
−2 Δ ln L
$c_{t\varphi}$ / Λ^2 [TeV-2]
CMS
138 fb-1 (13 TeV)
Observed
Expected
68% CL [-3.1, +4.9]
95% CL [-6.6, +8.7]
−2 Δ ln L
$c^{-}_{\varphi Q}$ / Λ^2 [TeV-2]

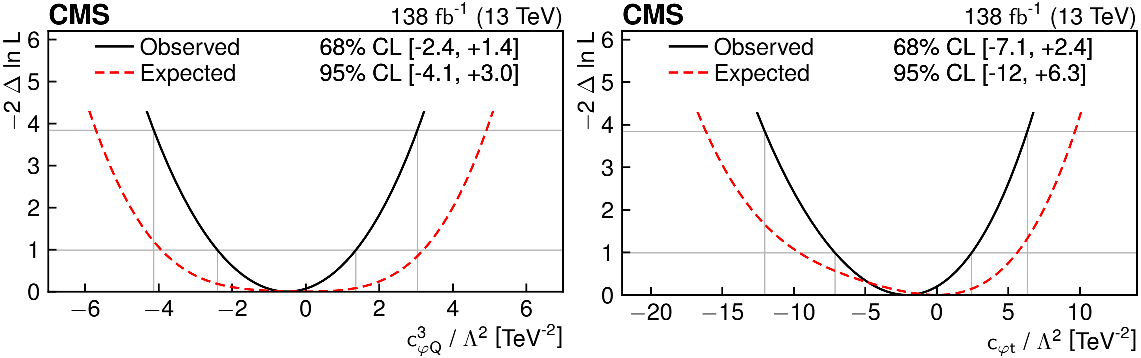
CMS
138 fb-1 (13 TeV)
Observed
Expected
68% CL [-2.4, +1.4]
95% CL [-4.1, +3.0]
−2 Δ ln L
$c^3_{\varphi Q}$ / Λ^2 [TeV-2]
CMS
138 fb-1 (13 TeV)
Observed
Expected
68% CL [-7.1, +2.4]
95% CL [-12, +6.3]
−2 Δ ln L
$c_{\varphi t}$ / Λ^2 [TeV-2]

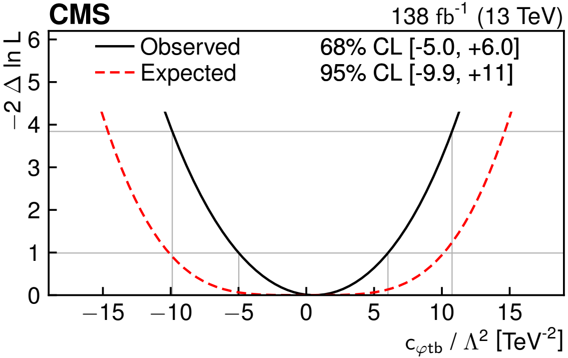
CMS
138 fb-1 (13 TeV)
Observed
Expected
68% CL [-5.0, +6.0]
95% CL [-9.9, +11]
−2 Δ ln L
0
1
2
3
4
5
6
−15
−10
−5
0
5
10
15
$c_{\varphi tb}$ / Λ^2 [TeV-2]

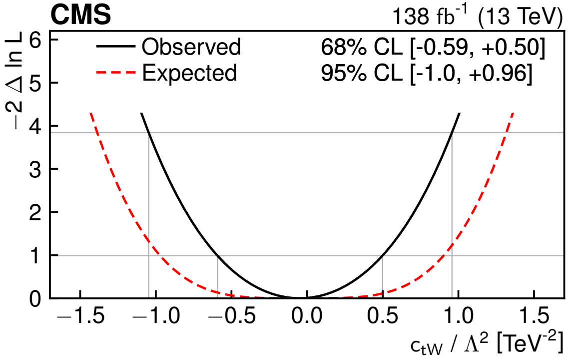
CMS
138 fb-1 (13 TeV)
Observed
Expected
68% CL [-0.59, +0.50]
95% CL [-1.0, +0.96]
−2 Δ ln L
0
1
2
3
4
5
6
−1.5
−1.0
−0.5
0.0
0.5
1.0
1.5
c_{tW} / Λ^2 [TeV-2]

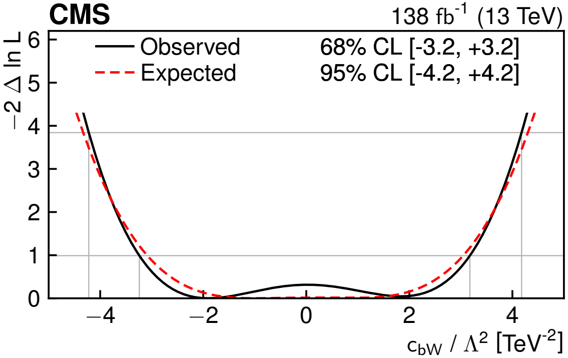
CMS
138 fb-1 (13 TeV)
Observed
Expected
68% CL [-3.2, +3.2]
95% CL [-4.2, +4.2]
−2 Δ ln L
cbW / Λ2 [TeV-2]

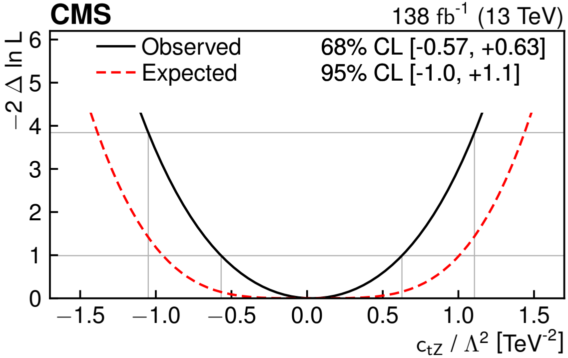
CMS
138 fb-1 (13 TeV)
Observed
Expected
68% CL [-0.57, +0.63]
95% CL [-1.0, +1.1]
−2 Δ ln L
ctZ / Λ2 [TeV-2]

WC summary

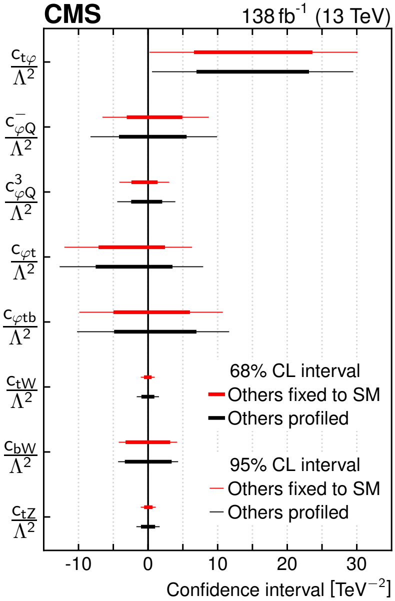
CMS
138 fb^{-1} (13 TeV)
$\frac{c_{t\varphi}}{\Lambda^2}$
$\frac{c^{-}_{\varphi Q}}{\Lambda^2}$
$\frac{c^{3}_{\varphi Q}}{\Lambda^2}$
$\frac{c_{\varphi t}}{\Lambda^2}$
$\frac{c_{\varphi tb}}{\Lambda^2}$
$\frac{c_{tW}}{\Lambda^2}$
$\frac{c_{bW}}{\Lambda^2}$
$\frac{c_{tZ}}{\Lambda^2}$
68% CL interval
Others fixed to SM
Others profiled
95% CL interval
Others fixed to SM
Others profiled
-10
0
10
20
30
Confidence interval [TeV^{-2}]

WC/Λ^2 [TeV^{-2}]	95% CL interval (others profiled)	95% CL interval (others fixed to SM)
$c_{t\varphi}$	[0.70, 29.42]	[0.31, 29.94]
$c_{\varphi Q}^{-}$	[−6.71, 7.72]	[−4.77, 5.54]
$c_{\varphi Q}^{3}$	[−4.01, 3.61]	[−3.86, 2.90]
$c_{\varphi t}$	[−10.91, 7.42]	[−8.32, 5.34]
$c_{\varphi tb}$	[−9.39, 10.65]	[−9.39, 10.12]
c_{tW}	[−1.56, 1.44]	[−1.02, 0.92]
c_{bW}	[−4.60, 4.57]	[−4.54, 4.47]
c_{tZ}	[−1.53, 1.46]	[−0.99, 1.00]

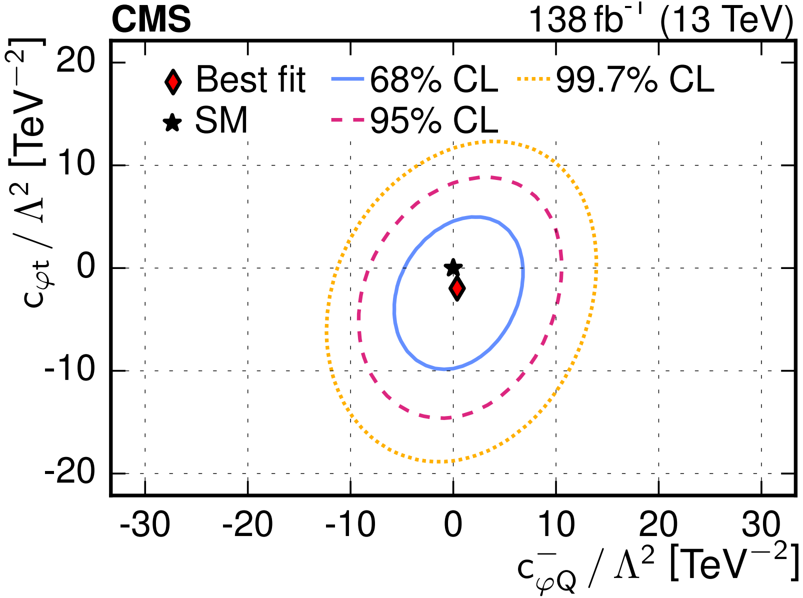
CMS
138 fb⁻¹ (13 TeV)
Best fit
68% CL
99.7% CL
SM
95% CL
$c_{\varphi t} / \Lambda^2$ [TeV^{-2}]
$c^{-}_{\varphi Q} / \Lambda^2$ [TeV^{-2}]
20
10
0
-10
-20
-30
-20
-10
0
10
20
30

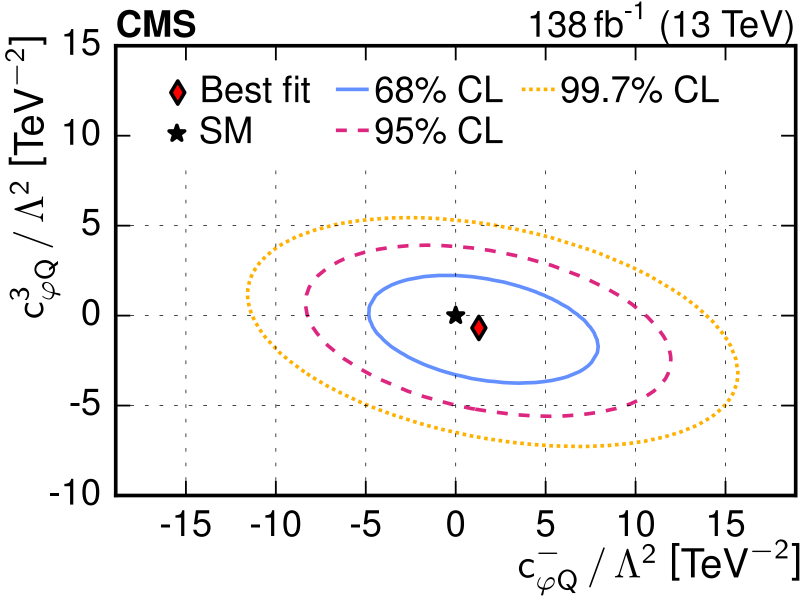
CMS
138 fb^{-1} (13 TeV)
Best fit
SM
68% CL
95% CL
99.7% CL
$c^{3}_{\varphi Q} / \Lambda^2$ [TeV^{-2}]
$c^{-}_{\varphi Q} / \Lambda^2$ [TeV^{-2}]
15
10
5
0
-5
-10
-15
-10
-5
0
5
10
15

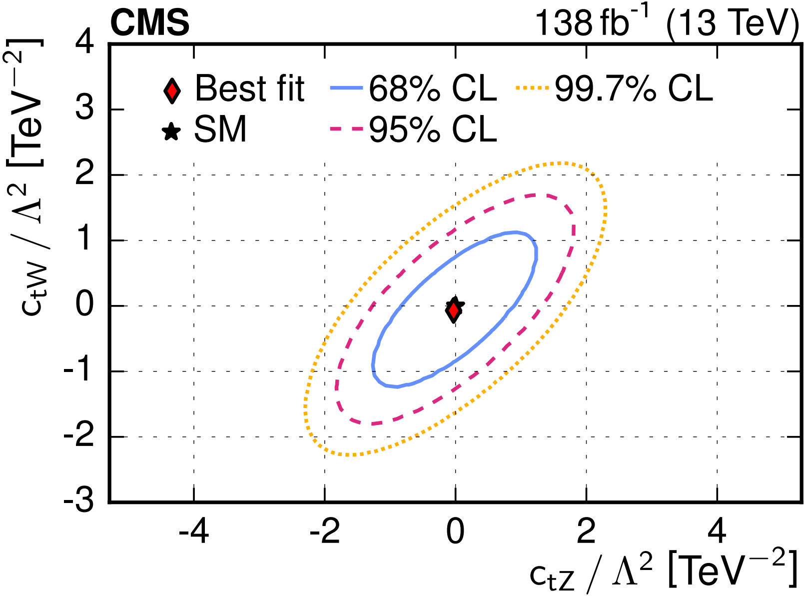
CMS
138 fb-1 (13 TeV)
Best fit
SM
68% CL
95% CL
99.7% CL
4
3
2
1
0
-1
-2
-3
-4
-2
0
2
4
c_{tW} / Λ^2 [TeV^{-2}]
c_{tZ} / Λ^2 [TeV^{-2}]

Name	Description
$t\bar{t}$ system	
b p_T	p_T of the leading (subleading) b jet
b score	DeepCSV score of the leading (subleading) b jet
q p_T	p_T of the leading (subleading) non-b jet
q score	DeepCSV score of the leading (subleading) non-b jet
$\Delta R(\mathrm{b},\mathrm{q})$	minimum ΔR between the leading (subleading) b jet and any non-b jet
$\Delta R(\mathrm{q},\mathrm{q})$	ΔR between the non-b jets closest and next-to-closest to the leading (subleading) b jet
$m(\mathrm{q}+\mathrm{q})$	invariant mass of the non-b jets closest and next-to-closest to the leading (subleading) b jet
$\Delta R(\mathrm{b},\mathrm{q}+\mathrm{q})$	ΔR between the leading (subleading) b jet and the sum of the nearest and next-to-nearest non-b jets
$m(\mathrm{b}+\mathrm{q}+\mathrm{q})$	invariant mass of the leading (subleading) b jet and the nearest and next-to-nearest non-b jets
$\Delta R(\mathrm{Z/H},\mathrm{b}+\mathrm{q}+\mathrm{q})$	ΔR between the Z/H boson candidate and the sum of the leading (subleading) b jet and the non-b jets nearest and next-to-nearest to the leading (subleading) b jet
$\Delta R(\mathrm{Z/H},\mathrm{b}+\mathrm{b}+\mathrm{q}+\mathrm{q}+\ell)$	ΔR between the Z/H boson candidate and the sum of the leading and subleading b jets, the non-b jets nearest and next-to-nearest to the leading (subleading) b jet, and the lepton
$m_T(\mathrm{b}+\ell+\vec{p}_T^{\,\mathrm{miss}})$	transverse mass of the subleading b jet, the lepton, and $\vec{p}_T^{\,\mathrm{miss}}$
$m(\mathrm{Z/H}+\mathrm{b})$	invariant mass of the Z/H boson candidate and the nearest b jet
$m(\mathrm{b}+\mathrm{b})$	invariant mass of the leading and subleading b jets
$\Delta R(\mathrm{b},\mathrm{b})$	ΔR between the leading and subleading b jets
$\Delta R(\mathrm{Z/H},\mathrm{q})$	ΔR between the Z/H boson candidate and the leading non-b jet
$\Delta R(\mathrm{Z/H},\mathrm{b})$	ΔR between the Z/H boson candidate and the leading b jet
$\Delta R(\mathrm{Z/H},\ell)$	ΔR between Z/H boson candidate and the lepton
$m(\mathrm{Z/H}+\ell)$	invariant mass of the Z/H boson candidate and the lepton
$\Delta R(\mathrm{b},\ell)$	ΔR between the leading (subleading) b jet and the lepton
$m(\mathrm{b}+\ell)$	invariant mass of the leading (subleading) b jet and the lepton
$N(\mathrm{b_{out}})$	number of b jets outside the Z/H boson candidate cone ($\Delta R > 0.8$)
$N(\mathrm{q_{out}})$	number of non-b jets outside the Z/H boson candiate cone ($\Delta R > 0.8$)
Event topology	
N(AK8 jets)	number of AK8 jets including the Z/H boson candidate
N(AK4 jets)	number of AK4 jets
N(Z/H)	number of AK8 jets with a minimum AK8 $\mathrm{b\bar{b}}$ tagger score of 0.8
AK8 m_{SD}	maximum m_{SD} of AK8 jets excluding the Z/H boson candidate
$H_T(\mathrm{b_{out}})$	H_T of the b jets outside the Z/H boson candidate cone ($\Delta R > 0.8$)
$H_T(\mathrm{b_{out}},\mathrm{q_{out}},\ell)$	H_T of all AK4 jets outside the Z/H boson candidate cone ($\Delta R > 0.8$) and the lepton
sphericity	sphericity calculated from the AK4 jets and the lepton **[?]**
aplanarity	aplanarity calculated from the AK4 jets and the lepton **[?]**
Z/H boson candidate substructure	
$\mathrm{b_{in}}$ score	maximum (minimum) DeepCSV score of AK4 jets within the Z/H boson candidate cone ($\Delta R \leq 0.8$)
$\Delta R(\mathrm{b_{in}},\mathrm{b_{out}})$	ΔR between a b jet within the Z/H boson candidate cone ($\Delta R \leq 0.8$) and the leading b jet outside of the Z/H boson candidate cone ($\Delta R > 0.8$)
$N(\mathrm{b_{in}})$	number of b jets within the Z/H boson candidate cone ($\Delta R \leq 0.8$)
$N(\mathrm{q_{in}})$	number of non-b jets within the Z/H boson candidate cone ($\Delta R \leq 0.8$)
Z/H $\mathrm{b\bar{b}}$ score	AK8 $\mathrm{b\bar{b}}$ tagger score of the Z/H boson candidate

Backup: $t\bar{t}\gamma$

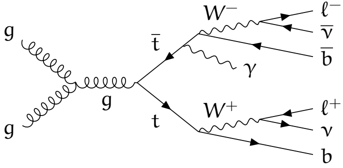
g
g
g
t̄
t
W⁻
W⁺
γ
ℓ⁻
ν̄
b̄
ℓ⁺
ν
b
q
q̄
g
γ
t̄
t
W⁻
W⁺
ℓ⁻
ν̄
b̄
ℓ⁺
ν
b
g
g
g
t̄
t
W⁻
W⁺
γ
ℓ⁻
ν̄
b̄
ℓ⁺
ν
b

Kinematic plots signal region

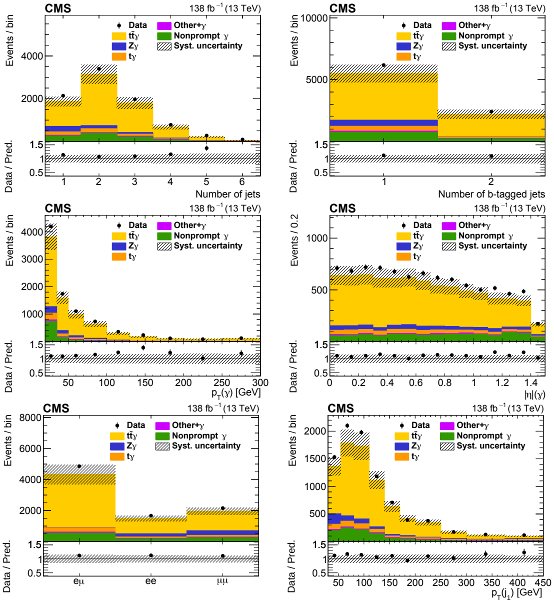

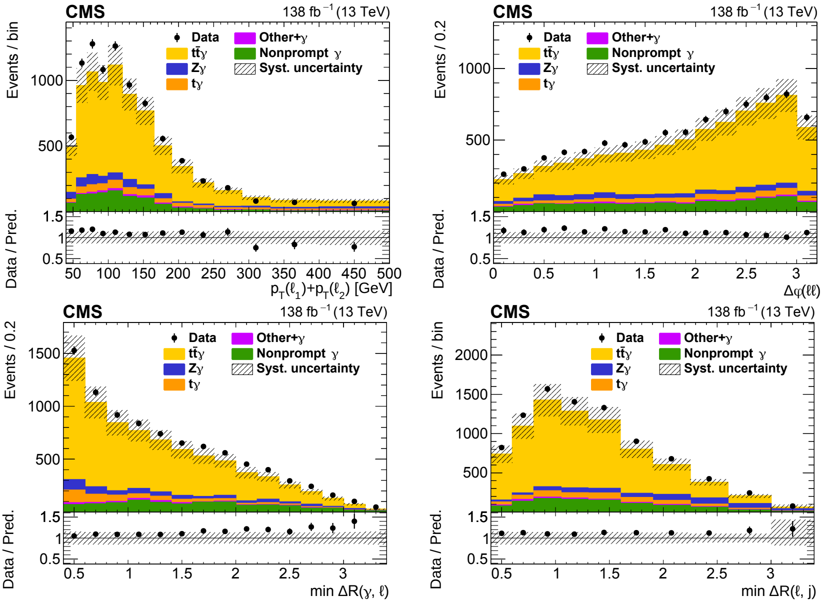

CMS
138 fb^{-1} (13 TeV)
Data
Other+γ
tt̄γ
Nonprompt γ
Zγ
Syst. uncertainty
tγ
Events / bin
Events / 0.2
Data / Pred.
$p_T(\ell_1)+p_T(\ell_2)$ [GeV]
$\Delta\varphi(\ell\ell)$
min $\Delta R(\gamma, \ell)$
min $\Delta R(\ell, j)$

Kinematic plots: Z gamma region

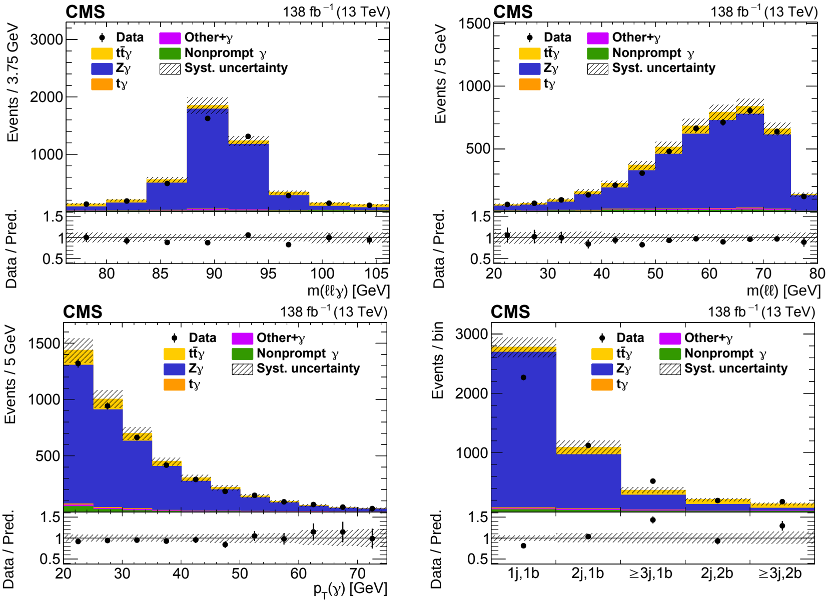

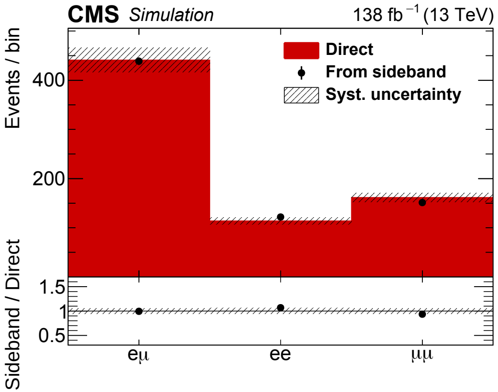
CMS Simulation
138 fb^{-1} (13 TeV)
Direct
From sideband
Syst. uncertainty
Events / bin
Sideband / Direct
400
200
1.5
1
0.5
eμ
ee
μμ

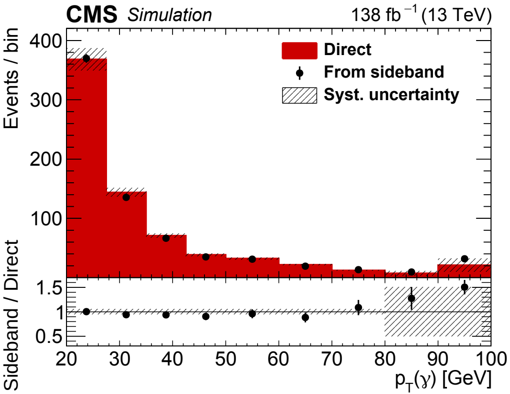
CMS Simulation
138 fb^{-1} (13 TeV)
Direct
From sideband
Syst. uncertainty
Events / bin
Sideband / Direct
400
300
200
100
1.5
1
0.5
20
30
40
50
60
70
80
90
100
$p_T(\gamma)$ [GeV]

photon pT in signal region

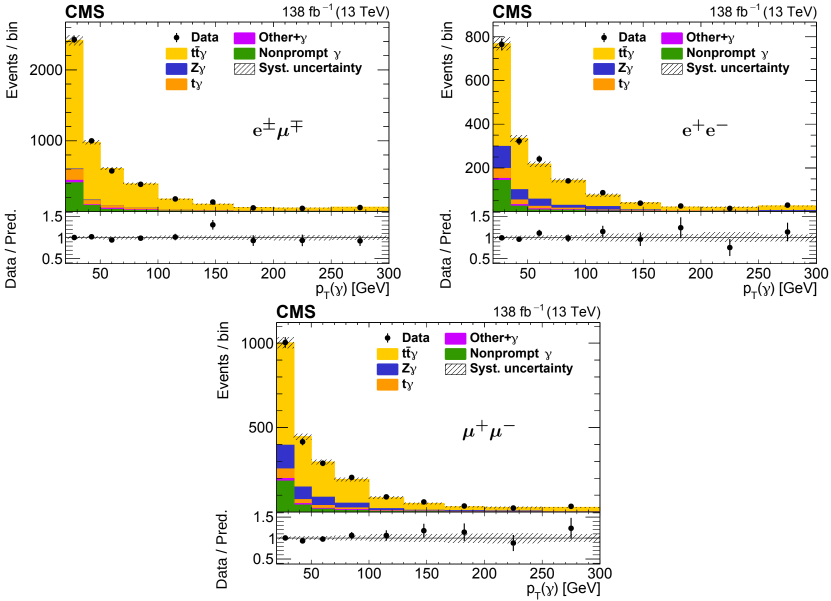

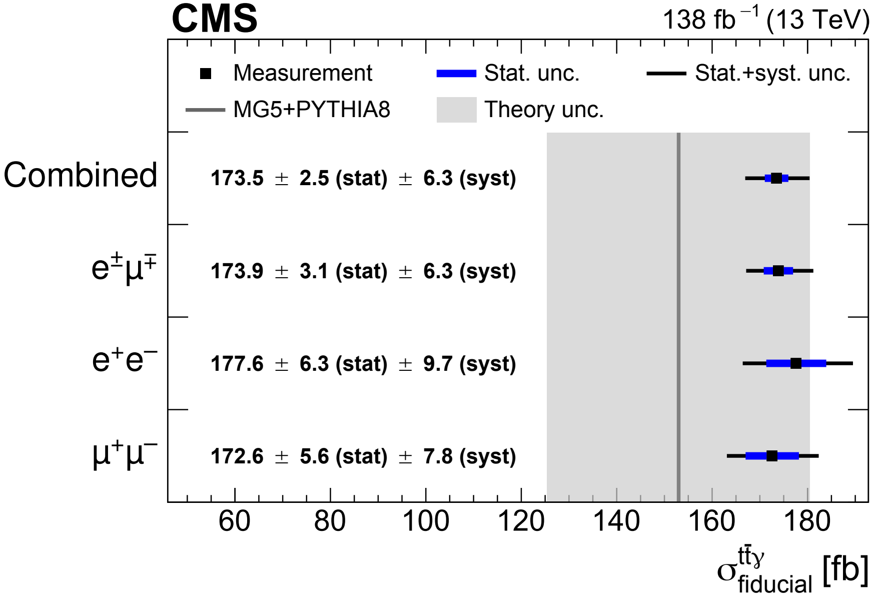
CMS
138 fb^{-1} (13 TeV)
Measurement
Stat. unc.
Stat.+syst. unc.
MG5+PYTHIA8
Theory unc.
Combined
173.5 ± 2.5 (stat) ± 6.3 (syst)
$e^{\pm}\mu^{\mp}$
173.9 ± 3.1 (stat) ± 6.3 (syst)
$e^{+}e^{-}$
177.6 ± 6.3 (stat) ± 9.7 (syst)
$\mu^{+}\mu^{-}$
172.6 ± 5.6 (stat) ± 7.8 (syst)
60
80
100
120
140
160
180
$\sigma^{t\bar{t}\gamma}_{\text{fiducial}}$ [fb]

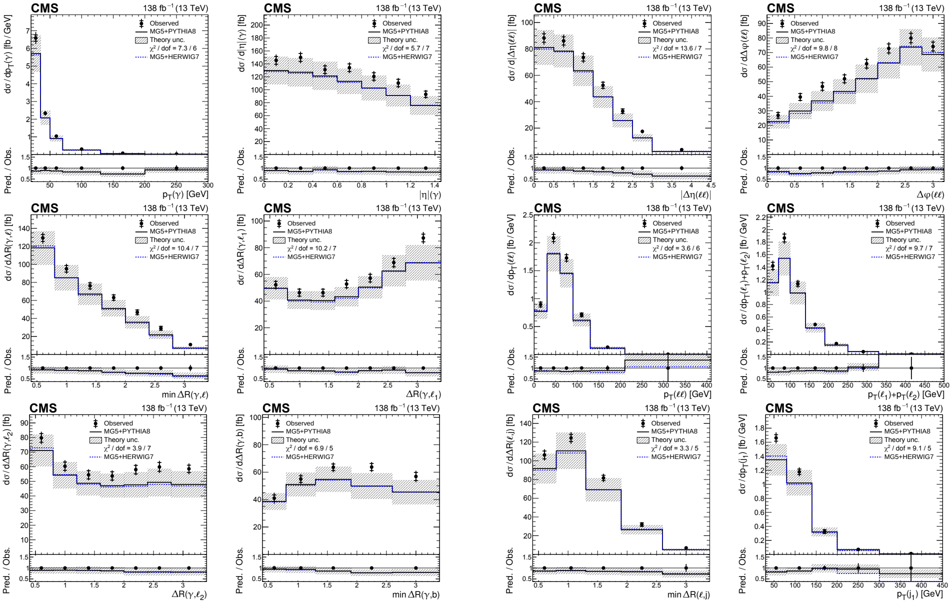
CMS
138 fb^{-1} (13 TeV)
Observed
MG5+PYTHIA8
Theory unc.
MG5+HERWIG7
χ^2 / dof = 7.3 / 6
χ^2 / dof = 5.7 / 7
χ^2 / dof = 13.6 / 7
χ^2 / dof = 9.8 / 8
χ^2 / dof = 10.4 / 7
χ^2 / dof = 10.2 / 7
χ^2 / dof = 3.6 / 6
χ^2 / dof = 9.7 / 7
χ^2 / dof = 3.9 / 7
χ^2 / dof = 6.9 / 5
χ^2 / dof = 3.3 / 5
χ^2 / dof = 9.1 / 5
Pred. / Obs.
dσ / dp$_T$(γ) [fb / GeV]
p$_T$(γ) [GeV]
dσ / d|η|(γ) [fb]
|η|(γ)
dσ / d|Δη(ℓℓ)| [fb]
|Δη(ℓℓ)|
dσ / dΔφ(ℓℓ) [fb]
Δφ(ℓℓ)
dσ / dΔR(γ,ℓ) [fb]
min ΔR(γ,ℓ)
dσ / dΔR(γ,ℓ$_1$) [fb]
ΔR(γ,ℓ$_1$)
dσ / dp$_T$(ℓℓ) [fb / GeV]
p$_T$(ℓℓ) [GeV]
dσ / dp$_T$(ℓ$_1$)+p$_T$(ℓ$_2$) [fb / GeV]
p$_T$(ℓ$_1$)+p$_T$(ℓ$_2$) [GeV]
dσ / dΔR(γ,ℓ$_2$) [fb]
ΔR(γ,ℓ$_2$)
dσ / dΔR(γ,b) [fb]
min ΔR(γ,b)
dσ / dΔR(ℓ,j) [fb]
min ΔR(ℓ,j)
dσ / dp$_T$(j$_1$) [fb / GeV]
p$_T$(j$_1$) [GeV]

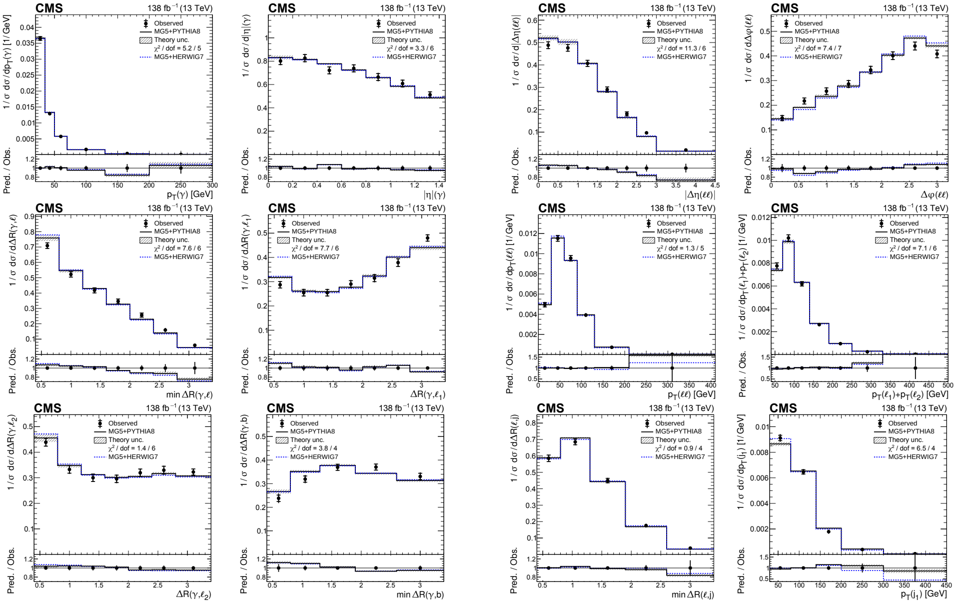
CMS
138 fb^{-1} (13 TeV)
Observed
MG5+PYTHIA8
Theory unc.
MG5+HERWIG7
χ^2 / dof = 5.2 / 5
χ^2 / dof = 3.3 / 6
χ^2 / dof = 11.3 / 6
χ^2 / dof = 7.4 / 7
χ^2 / dof = 7.6 / 6
χ^2 / dof = 7.7 / 6
χ^2 / dof = 1.3 / 5
χ^2 / dof = 7.1 / 6
χ^2 / dof = 1.4 / 6
χ^2 / dof = 3.8 / 4
χ^2 / dof = 0.9 / 4
χ^2 / dof = 6.5 / 4
Pred. / Obs.
$p_T(\gamma)$ [GeV]
$|\eta|(\gamma)$
$|\Delta\eta(\ell\ell)|$
$\Delta\varphi(\ell\ell)$
min $\Delta R(\gamma,\ell)$
$\Delta R(\gamma,\ell_1)$
$p_T(\ell\ell)$ [GeV]
$p_T(\ell_1)+p_T(\ell_2)$ [GeV]
$\Delta R(\gamma,\ell_2)$
min $\Delta R(\gamma,b)$
min $\Delta R(\ell,j)$
$p_T(j_1)$ [GeV]

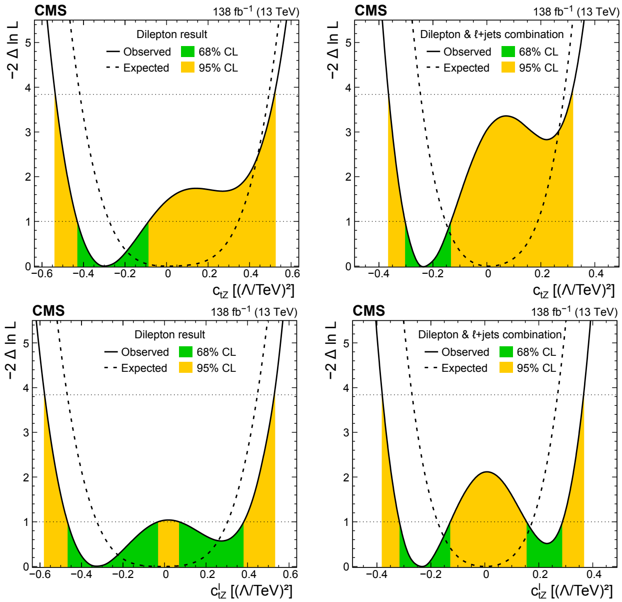
CMS
138 fb^{-1} (13 TeV)
Dilepton result
Observed
Expected
68% CL
95% CL
$-2\,\Delta\ln L$
c_{tZ} [$(\Lambda/\text{TeV})^2$]
Dilepton & ℓ+jets combination
c^{I}_{tZ} [$(\Lambda/\text{TeV})^2$]

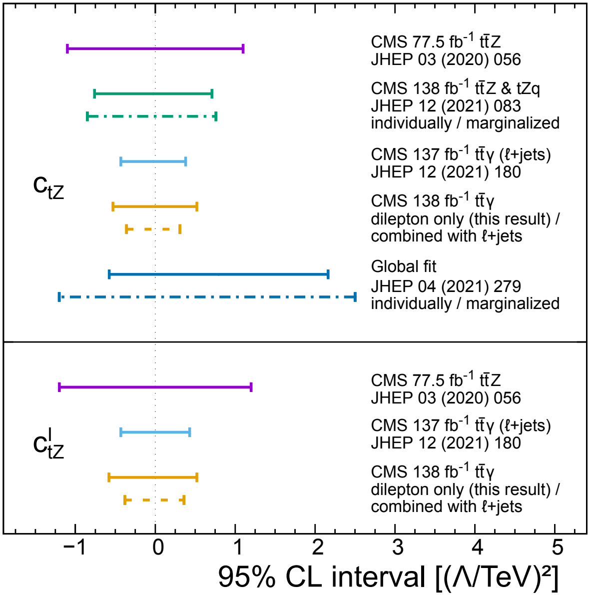
CMS 77.5 fb-1 tt̄Z
JHEP 03 (2020) 056
CMS 138 fb-1 tt̄Z & tZq
JHEP 12 (2021) 083
individually / marginalized
CMS 137 fb-1 tt̄γ (ℓ+jets)
JHEP 12 (2021) 180
CMS 138 fb-1 tt̄γ
dilepton only (this result) /
combined with ℓ+jets
Global fit
JHEP 04 (2021) 279
individually / marginalized
ctZ
CMS 77.5 fb-1 tt̄Z
JHEP 03 (2020) 056
CMS 137 fb-1 tt̄γ (ℓ+jets)
JHEP 12 (2021) 180
CMS 138 fb-1 tt̄γ
dilepton only (this result) /
combined with ℓ+jets
clₜZ
−1
0
1
2
3
4
5
95% CL interval [(Λ/TeV)²]

Process	Cross section normalization	Event generator	Perturbative order in QCD
$t\bar{t}\gamma$	NLO	MadGraph5_aMC@NLO	LO
Z+jets	NNLO [49]	MadGraph5_aMC@NLO	LO
Zγ, Wγ, VV, VVV, $t\bar{t}$V, tZq, tWZ, tHq, tHW, $t\bar{t}$VV, $t\bar{t}t\bar{t}$	NLO	MadGraph5_aMC@NLO	NLO
$t\bar{t}$	NNLO+NNLL [50]	POWHEG	NLO
single t (t channel)	NLO [51, 52]	POWHEG	NLO
single t (s channel)	NLO [51, 52]	MadGraph5_aMC@NLO	NLO
tW	NNLO [53]	POWHEG	NLO
$t\bar{t}$H	NLO	POWHEG	NLO
gg $\rightarrow$ ZZ	LO	MCFM	LO

Leptons	Photons	Jets	b jets	Events
$p_T > 25\,(15)\,\mathrm{GeV}$	$p_T > 20\,\mathrm{GeV}$	$p_T > 30\,\mathrm{GeV}$	$p_T > 30\,\mathrm{GeV}$	$N_\ell = 2$ (OC)
$\|\eta\| < 2.4$	$\|\eta\| < 1.44$	$\|\eta\| < 2.4$	$\|\eta\| < 2.4$	$N_\gamma = 1$
	$\Delta R(\gamma, \ell) > 0.4$	$\Delta R(\mathrm{jet}, \ell) > 0.4$	$\Delta R(\mathrm{jet}, \ell) > 0.4$	$N_\mathrm{b} \geq 1$
	isolated	$\Delta R(\mathrm{jet}, \gamma) > 0.1$	$\Delta R(\mathrm{jet}, \gamma) > 0.1$	$m(\ell\ell) > 20\,\mathrm{GeV}$
			matched to b hadron	

	Source	Correlation	Uncertainty [%] Prefit range	Postfit
Experimental	Integrated luminosity	$\sim$	1.3–3.2	1.7
	Pileup	✓	0.1–1.4	0.7
	Trigger efficiency	×	0.6–1.7	0.6
	Electron selection efficiency	$\sim$	1.0–1.3	1.0
	Muon selection efficiency	$\sim$	0.3–0.5	0.5
	Photon selection efficiency	$\sim$	0.4–3.6	1.1
	Electron & photon energy	✓	0.0–1.1	0.1
	Jet energy scale	$\sim$	0.1–1.3	0.5
	Jet energy resolution	✓	0.0–0.6	<0.1
	b tagging efficiency	$\sim$	0.9–1.4	1.1
	L1 prefiring	✓	0.0–0.8	0.3
Theoretical	Values of μ_F and μ_R	✓	0.3–3.5	1.3
	PDF choice	✓	0.3–4.5	0.3
	PS modelling: ISR & FSR scale	✓	0.3–3.5	1.3
	PS modelling: colour reconnection	✓	0.0–8.4	0.2
	PS modelling: b fragmentation	✓	0.0–2.2	0.7
	Underlying-event tune	✓	0.5	0.5
Background	$Z\gamma$ correction & normalization	✓	0.0–0.2	0.1
	$t\gamma$ normalization	✓	0.0–0.9	0.8
	Other+γ normalization	✓	0.3–1.0	0.8
	Nonprompt γ normalization	✓	0.0–1.8	0.7
	Size of simulated samples	×	1.5–7.6	0.9
	Total systematic uncertainty			3.6
	Statistical uncertainty			1.4
	Total uncertainty			3.9

Symbol	Definition
$p_{\mathrm{T}}(\gamma)$	Transverse momentum of the photon
$\|\eta\|(\gamma)$	Absolute value of the pseudorapidity of the photon
$\min \Delta R(\gamma, \ell)$	Angular separation between the photon and the closest lepton
$\Delta R(\gamma, \ell_1)$	Angular separation between the photon and the leading lepton
$\Delta R(\gamma, \ell_2)$	Angular separation between the photon and the subleading lepton
$\min \Delta R(\gamma, \mathrm{b})$	Angular separation between the photon and the closest b jet
$\|\Delta\eta(\ell\ell)\|$	Pseudorapidity difference between the two leptons
$\Delta\varphi(\ell\ell)$	Azimuthal angle difference between the two leptons
$p_{\mathrm{T}}(\ell\ell)$	Transverse momentum of the dilepton system
$p_{\mathrm{T}}(\ell_1) + p_{\mathrm{T}}(\ell_2)$	Scalar sum of the transverse momenta of the two leptons
$\min \Delta R(\ell, \mathrm{j})$	Smallest angular separation between any of the selected leptons and jets
$p_{\mathrm{T}}(\mathrm{j}_1)$	Transverse momentum of the leading jet

	Wilson coefficient		Dilepton result: 68% CL interval [$(\Lambda/\text{TeV})^2$]	Dilepton result: 95% CL interval [$(\Lambda/\text{TeV})^2$]	Dilepton & ℓ+jets combination: 68% CL interval [$(\Lambda/\text{TeV})^2$]	Dilepton & ℓ+jets combination: 95% CL interval [$(\Lambda/\text{TeV})^2$]
Expected	c_{tZ}	$c^I_{tZ} = 0$	$[-0.28, 0.35]$	$[-0.42, 0.49]$	$[-0.15, 0.19]$	$[-0.25, 0.29]$
		profiled	$[-0.28, 0.35]$	$[-0.42, 0.49]$	$[-0.15, 0.19]$	$[-0.25, 0.29]$
	c^I_{tZ}	$c_{tZ} = 0$	$[-0.33, 0.30]$	$[-0.47, 0.45]$	$[-0.17, 0.18]$	$[-0.27, 0.27]$
		profiled	$[-0.33, 0.30]$	$[-0.47, 0.45]$	$[-0.18, 0.18]$	$[-0.27, 0.27]$
Observed	c_{tZ}	$c^I_{tZ} = 0$	$[-0.43, -0.09]$	$[-0.53, 0.52]$	$[-0.30, -0.13]$	$[-0.36, 0.31]$
		profiled	$[-0.43, 0.17]$	$[-0.53, 0.51]$	$[-0.30, 0.00]$	$[-0.36, 0.31]$
	c^I_{tZ}	$c_{tZ} = 0$	$[-0.47, -0.03] \cup [0.07, 0.38]$	$[-0.58, 0.52]$	$[-0.32, -0.13] \cup [0.16, 0.29]$	$[-0.38, 0.36]$
		profiled	$[-0.43, 0.33]$	$[-0.56, 0.51]$	$[-0.28, 0.23]$	$[-0.36, 0.35]$

Backup: Charged lepton flavor violation

Vertex	Int. type	Cross section [fb] Exp	Cross section [fb] Obs	$C_{e\mu tq}/\Lambda^2$ [TeV $^{-2}$] Exp	$C_{e\mu tq}/\Lambda^2$ [TeV $^{-2}$] Obs	$\mathcal{B}(10^{-6})$ Exp	$\mathcal{B}(10^{-6})$ Obs
$e\mu tu$	Vector	7.02	6.78	0.12	0.12	0.14	0.13
	Scalar	5.63	6.25	0.23	0.24	0.06	0.07
	Tensor	10.01	9.18	0.07	0.06	0.27	0.25
$e\mu tc$	Vector	11.21	9.73	0.39	0.37	1.49	1.31
	Scalar	9.11	8.88	0.87	0.86	0.91	0.89
	Tensor	21.02	17.22	0.24	0.21	3.16	2.59

- No sign of charged lepton flavor violation
- Set limits on cross sections
- Scalar, vector, tensor contribute differently to production vs. decay
- Scalar cross section limits strongest, tensor weakest
- Translate into branching ratio exclusions
- Excluded region above and right of curves

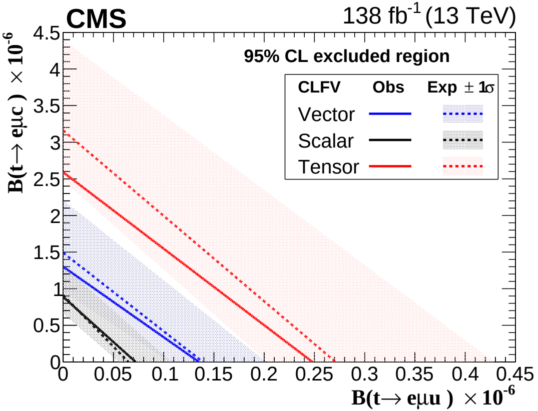

- Near-degeneracy of BDT shapes makes exclusion curves nearly straight lines

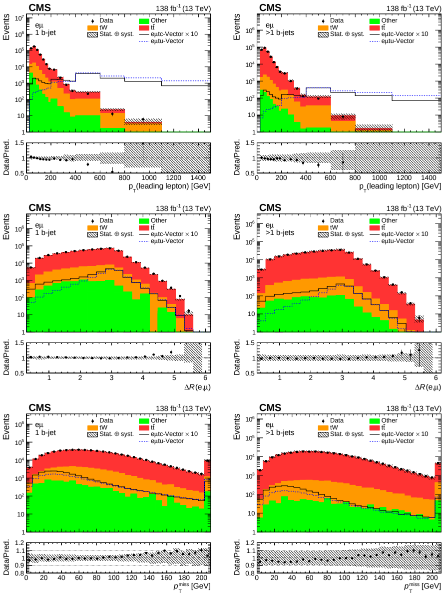
CMS
138 fb-1 (13 TeV)
Data
Other
tW
tt̄
Stat. ⊕ syst.
eμtc-Vector × 10
eμtu-Vector
eμ
1 b-jet
>1 b-jets
Events
Data/Pred.
p_T(leading lepton) [GeV]
ΔR(e,μ)
p_T^miss [GeV]

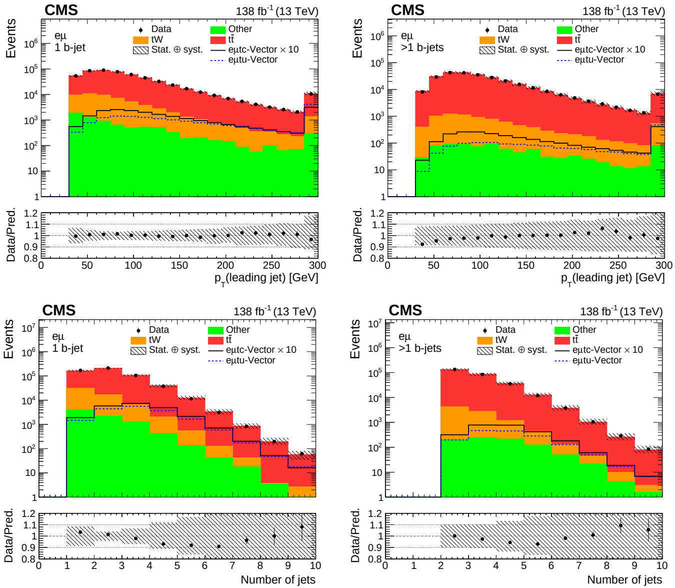
CMS
138 fb-1 (13 TeV)
Events
eμ
1 b-jet
Data
Other
tW
tt̄
Stat. ⊕ syst.
eμtc-Vector × 10
eμtu-Vector
Data/Pred.
p_T(leading jet) [GeV]
CMS
138 fb-1 (13 TeV)
eμ
>1 b-jets
p_T(leading jet) [GeV]
CMS
138 fb-1 (13 TeV)
eμ
1 b-jet
Number of jets
CMS
138 fb-1 (13 TeV)
eμ
>1 b-jets
Number of jets

BDT outputs

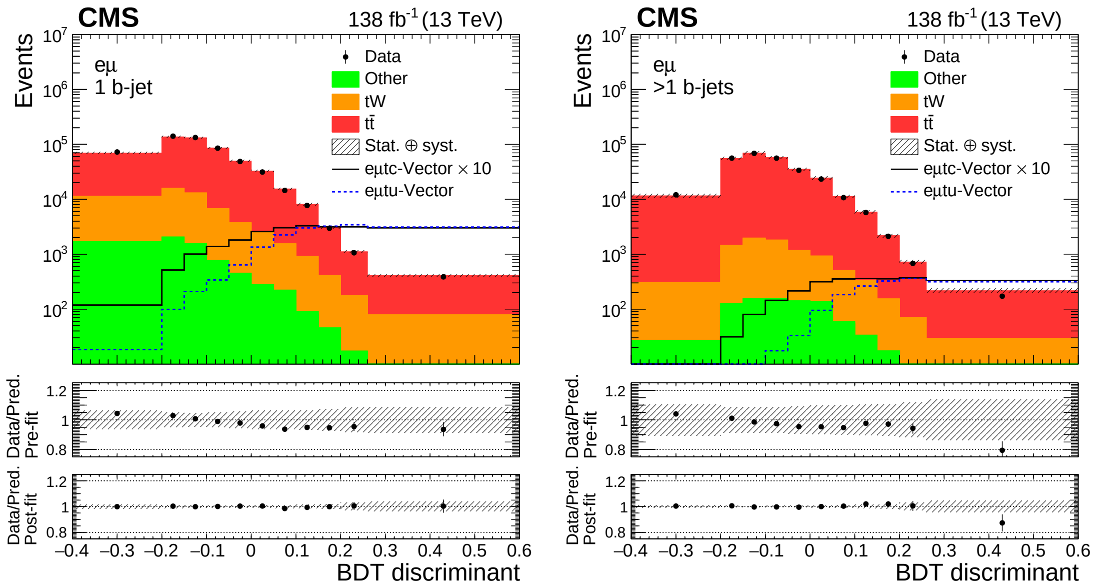
CMS
138 fb^{-1} (13 TeV)
eμ
1 b-jet
Data
Other
tW
$t\bar{t}$
Stat. ⊕ syst.
eμtc-Vector × 10
eμtu-Vector
Events
Data/Pred. Pre-fit
Data/Pred. Post-fit
BDT discriminant
CMS
138 fb^{-1} (13 TeV)
eμ
>1 b-jets
BDT discriminant

Channel			1 b tagged	> 1 b tagged
$t\bar{t}$			477800 ± 7900	265000 ± 7100
tW			49100 ± 1300	7710 ± 250
Other			7950 ± 670	850 ± 70
Total background prediction			534900 ± 8000	273600 ± 7100
Data			537236	268781
$e\mu tu$	Vector	t decay	604 ± 2	45.2 ± 0.4
		t production	17103 ± 29	1557 ± 9
	Scalar	t decay	78.2 ± 0.2	6.1 ± 0.1
		t production	3670 ± 6	336 ± 2
	Tensor	t decay	3499 ± 9	266 ± 2
		t production	61011 ± 107	5567 ± 33
$e\mu tc$	Vector	t decay	596 ± 2	90.4 ± 0.5
		t production	1711 ± 3	166 ± 1
	Scalar	t decay	77.7 ± 0.2	11.4 ± 0.1
		t production	294 ± 1	28.5 ± 0.2
	Tensor	t decay	3467 ± 8	534 ± 3
		t production	6329 ± 13	621 ± 4

Source	$t\bar{t}$ (%)	CLFV signal	
		decay (%)	production (%)
Trigger	1.2	1.2	2.9
Electron identification and isolation	1.6	1.6	3.9
Muon identification and isolation	0.6	0.6	0.7
Electron energy scale and resolution	<0.1	<0.1	<0.1
Muon momentum scale and resolution	<0.1	<0.1	<0.1
Jet energy scale and resolution	2.5	2.1	1.2
b tagging	3.1	3.9	4.5
Pileup	0.3	0.3	0.2
ME scale	0.9	0.8	0.7
ISR/FSR scale	1.5	2.9	1.9
PDF	0.8	0.8	0.9
UE tune	0.4	—	—
ME/PS matching	<0.1	—	—
Color reconnection	1.0	—	—
MC statistical	<0.1	<0.1	<0.1